Department of Pathology
Department of Surgery
Translational Cancer Biology, Research Programs Unit
University of Helsinki
Finland

Biomarkers in pheochromocytomas and paragangliomas

Helena Leijon

ACADEMIC DISSERTATION

To be presented, with the permission of the Faculty of Medicine of the University of Helsinki, for public examination at small auditorium, Haartman Institute on December 21th 2018 at 12 noon

Helsinki 2018

Supervised by

Professor Johanna Arola, M.D., Ph.D.
Department of Pathology, University of Helsinki
Helsinki University Hospital, Helsinki, Finland

Professor Caj Haglund, M.D., Ph.D.
Department of Surgery, University of Helsinki
Helsinki University Hospital, Helsinki, Finland

Docent Kaisa Salmenkivi, M.D., Ph.D.
Department of Pathology, University of Helsinki
Helsinki University Hospital, Helsinki, Finland

Reviewed by

Professor Tuomo Karttunen, M.D., Ph.D.
Department of Pathology, University of Oulu and
Oulu University Hospital, Oulu, Finland

Professor Raimo Voutilainen, M.D., Ph.D.
Department of Pediatrics, University of Eastern Finland
Kuopio University Hospital, Kuopio, Finland.

Opposed by

Docent Paula Kujala, M.D., Ph.D.
Department of Pathology, Fimlab Laboratories,
Tampere University Hospital, Tampere,
and University of Turku, Turku, Finland

ISBN 978-951-51-4750-9 (pbk)
ISBN 978-951-51-4751-6 (PDF)

http://ethesis.helsinki.fi

Unigrafia
Helsinki 2018

Contents

Contents 3

1 List of original publications 6

2 Abbreviations 7

3 Abstract 9

4 Introduction 11

5 Review of the literature 12

5.1 Adrenal gland and paraganglion system 12

5.1.1 Adrenal gland 12

5.1.2 Paraganglion system 15

5.2 Pheochromocytomas and paragangliomas 16

5.2.1 Epidemiology and risk factors 16

5.2.2 Genetic basis, pathogenesis, and most important associated syndromes 17

5.2.3 Somatostatin receptor expression in pheochromocytomas and paragangliomas 23

5.2.4 Clinical presentation 24

5.2.5 Diagnosis 27

5.2.6 Treatment 30

5.2.7 Gross appearance and histopathology 33

5.2.8 Immunohistochemistry and differential diagnosis 36

5.2.9 Metastatic pheochromocytomas and paragangliomas and factors associated with metastatic potential 38

5.2.10. Posttranslational modifications of proteins 41

6 Aims of the study 45

7 Material and methods 46

7.1 Patient cohorts, tissue samples, and histopathological parameters 46
7.2 Tissue microarray blocks 47
7.3 Immunohistochemistry and scoring 48
7.4 Mass spectrometric N-glycan profiling 50
7.5 Genetic analysis 50
7.6 Statistical analysis 51
7.7 Approvals 52
8 Results 53
8.1 Clinical, histopathological data, and proliferation (Studies I and II) 53
8.2 Immunohistochemistry results 54
8.2.1 Human antigen R protein (Study I) 54
8.2.2 Somatostatin receptors in pheochromocytomas and paragangliomas (Study II) 55
8.2.3 SDHB and SDHA immunohistochemistry expression (Studies II and III) 58
8.3 Glycomics (Study III) 58
8.3.1 Neutral and acidic asparagine-linked glycan profiles 59
8.3.2 Principal component analysis 60
8.4 Thyroid paragangliomas (Study IV) 62
8.4.1 Clinical characteristics 62
8.4.2 Histology and immunohistochemistry in thyroid paragangliomas 63
8.4.3 Molecular genetic results 63
9 Discussion 64
10 Conclusions 69
11 Acknowledgments 70
12 References 73

1 List of original publications

This thesis is based on the following publications:

I Leijon H, Salmenkivi K, Heiskanen I, Hagström J, Louhimo J, Heikkilä P, Ristimäki A, Paavonen T, Metso S, Mäenpää H, Haglund C and Arola J: HuR in pheochromocytomas and paragangliomas – overexpression in verified malignant tumors. APMIS 124(9):757-63, 2016

II Leijon H, Remes S, Hagström J, Louhimo J, Mäenpää H, Schalin-Jäntti C, Miettinen M, Haglund C and Arola J: Variable SSTR subtype expression in 151 primary pheochromocytomas and paragangliomas. Human Pathology, in press

III Leijon H, Kaprio T, Heiskanen A, Satomaa T, Hiltunen JO, Miettinen MM, Arola J, Haglund C: N-glycomic profiling of pheochromocytomas and paragangliomas separates metastatic and non-metastatic disease. J Clin Endocrinol Metab 102(11):3990-4000, 2017

IV von Dobschuetz E, Leijon H, Schalin-Jäntti C, Schiavi F, Brauckhoff M, Peczkowska M, Spiazzi G, Dematte S, Cecchini ME, Sartorato P, et al.: A registry-based study of thyroid paraganglioma: histological and genetic characteristics. Endocr Relat Cancer 22(2):191-204, 2015

The publications are referred to in the text by their roman numerals.

2 Abbreviations

ACTH	adrenocorticotropic hormone
AKT	protein kinase B
ARE	adenylate/uridylate rich element
ATP	adenosine triphosphate
cAMP	cyclic adenosine monophosphate
COX	cyclooxygenase
CRH	corticotrophin-releasing hormone
CSDE1	cold shock domain containing E1
CT	computed tomography
DHEA	dehydroepiandrosterone
DHEAS	dehydroepiandrosterone sulfate
EGF	epidermal growth factor
ER	estrogen receptor
ERK	extracellular signal-regulated kinase
FH	fumarate hydratase
FNA	fine-needle aspiration
GAPP	Grading of Adrenal Pheochromocytoma and Paraganglioma
GATA3	trans-acting T-cell-specific transcription factor
GFAP	glial fibrillary acidic protein
GIST	gastrointestinal stromal tumor
GM-CSF	granulocyte-macrophage colony-stimulating factor
HIF	hypoxia-inducible factor
HNPGL	head and neck paraganglioma
HPF	high power field
HU	Hounsfield unit
HuR	human antigen R
IHC	immunohistochemistry
IL-6	interleukin-6
IL-13	interleukin-13
iNOS	inducible NO synthase
KIF1B	kinesin family member 1B
MALDI-TOF	matrix-assisted laser desorption/ionization- time of flight
MAML3	mastermind-like transcriptional coactivator 3
MAX	Myc-associated factor X
MDH2	malate dehydrogenase
MEN2	multiple endocrine neoplasia type 2
MGMT	O-methylguanine-DNA methyltransferase

MIB1	antibody against Ki-67
MIBG	metaiodobenzylguanidine
MMP-9	matrix metalloproteinase-9
MRI	magnetic resonance imaging
MTC	medullary thyroid carcinoma
mTOR	mammalian target of rapamycin
NET	neuroendocrine tumor
NF1	neurofibromatosis 1
NSE	neuron-specific enolase
PA	pituitary adenoma
PASS	Pheochromocytoma of the Adrenal Gland Scaled Score
PCA	principal component analysis
PCR	polymerase chain reaction
PD-1	programmed cell death protein 1
PET	positron emission tomography
PGL	paraganglioma
PHEO	pheochromocytoma
Prot α	prothymosin α
PRRT	peptide receptor radionuclide therapy
RBP	RNA-binding protein
RCC	renal cell carcinoma
RET	rearranged during transfection
RRM	RNA recognition motif
SDH	succinate dehydrogenase
SDHB	succinate dehydrogenase subunit B
SPECT	single-photon emission computed tomography
SSTR	somatostatin receptor
TCA	tricarboxylic acid
TGF-β	transforming growth factor-β
TLR4	toll-like receptor-4
TMA	tissue microarray
TMEM127	transmembrane protein 127
TNF-α	tumor necrosis factor-α
TSP-1	thrombospondin 1
UBTF	upstream binding transcription factor
uPA	urokinase-type plasminogen activator
uPAR	urokinase-type plasminogen activator receptor
VEGF	vascular endothelial growth factor
VHL	von Hippel–Lindau

3 Abstract

Pheochromocytomas (PHEOs) derived from adrenal medulla and paragangliomas (PGLs) from sympathetic or parasympathetic paraganglia are rare neuroendocrine tumors. Incidence of PHEOs and PGLs is between 0.4–9.5 cases per one million people per year. In Finland about 10–15 PHEOs are diagnosed per year, but the incidence is rising. Sympathetic PGLs occur about one tenth as often as PHEOs, and parasympathetic PGLs constitute about 20% of PGLs. PHEOs and sympathetic PGLs can secrete catecholamines, often in bouts, which makes the symptoms associated with these tumors very diverse, with high blood pressure being the leading symptom.

During recent years, knowledge of the variable genetic background and pathogenesis of PGLs and PHEOs has increased, and about 30-40% of these tumors are known to be hereditary. However, prognosis and aggressiveness of an individual tumor cannot be unequivocally predicted histologically or with any biomarkers. The aim of this thesis was to find biomarkers in PHEOs and PGLs for diagnostic, prognostic, and predictive purposes. A special focus was the differences between metastatic and nonmetastatic tumors as well as between PGLs and PHEOs.

The study cohort consisted of 153 consecutive PHEOs or PGLs operated from 147 patients during the years 1973–2009 at Helsinki University Hospital. Clinical information was collected from hospital records, and tissue microarray blocks were constructed for immunohistochemistry studies. Matrix-assisted laser desorption/ionization time of flight mass spectrometric profiling of 16 tissue samples was used to analyze N-glycan structures in eight metastasized and eight nonmetastasized tumors. In addition, five thyroid PGLs originating from the population-based European-American-Head-and-Neck-Paraganglioma-Registry (European-American-HNPGL-Registry, Freiburg, Germany) were investigated. These PGL patients were tested for germ-line mutations of the genes, which have been associated with head and neck PGLs.

Metastasized PHEOs and PGLs expressed significantly more intracytoplasmic human antigen R (HuR) protein immunohistochemically than nonmetastasized tumors. HuR's target, cyclooxygenase-2 (COX-2), was increased in metastatic tumors too. The metastatic potential was also associated with higher proliferation and tumor necrosis. Five somatostatin receptors (SSTR1–5) showed individual and varying SSTR profiles in PHEOs and PGLs. The most abundant SSTRs were SSTR2 and SSTR3. Between metastatic PHEOs and PGLs the SSTR2 expression varied – all PGLs were strongly SSTR2 positive, while most PHEOs were negative. The metastatic tumors showed less SSTR3 positivity than the nonmetastatic ones.

The N-glycan profile differed depending on the metastatic status of the tumor. Metastasized tumors expressed more fucosylation and complex fucosylation in their N-glycans. Based on different N-glycan profiles, metastatic and nonmetastatic tumors and also PGLs and PHEOs could be separated in principal component analysis.

Extremely rare thyroid PGLs showed a strong association with succinate dehydrogenase *(SDH)* mutation. Of five patients with thyroid PGL, two had *SDHB* mutation and two *SDHA* mutation. In our Finnish cohort, 10% of PHEO and PGL patients had *SDHB* mutation and 40% of these a metastatic disease.

In conclusion, intracytoplasmic HuR is increased in most metastatic PHEOs and PGLs and can be used in the panel of prognostic markers in these tumors. HuR may have a role in malignant transformation. PHEOs and PGLs have individual variable SSTR1–5 profiles. Investigating the SSTR1–5 profile in PHEOs and PGLs can be beneficial in choosing somatostatin analog based imaging and therapy. Metastasized and nonmetastasized PHEOs and PGLs have differences in N-glycans. Those N-glycans, associated with aggressive disease, may possibly be used in the future as prognostic biomarkers. PHEOs and PGLs have a strong genetic background, and genetic testing is recommended for PHEO and PGL patients.

4 Introduction

Pheochromocytomas (PHEOs) and paragangliomas (PGLs) are rare neuroendocrine tumors that are embryonically derived from the neural crest. Tumors that develop from the adrenal medulla are called pheochromocytomas. Histologically similar tumors that develop from sympathetic or parasympathetic paraganglia are called paragangliomas (Tischler 2008). Tumors originating from sympathetic cells, also called chromaffin cells, often secrete catecholamines leading to diverse symptoms related to catecholamine excess. Parasympathetic PGLs do not usually secrete catecholamines (Lenders et al. 2014, Davison et al. 2018).

The name pheochromocytoma comes from the Greek *phaios* meaning "dark," *chroma* meaning "color," and *cytom* meaning "tumor" (Bausch et al. 2017, Sane 2009). The word "chromaffin" comes from *chrom*ium and *affin*ity. Chromaffin cells can be visualized by staining with chromium salts, which oxidize catecholamines to form a brown color (Bausch et al. 2017).

Diagnosis of PHEOs and PGLs is still a challenge both to clinicians and to pathologists, although knowledge has increased a lot during recent decades. New prognostic markers associated with metastatic potential are needed. The leading symptom of these tumors is high blood pressure, paroxysmal or sustained, but the symptoms can vary and therefore this tumor has been called a great mimicker (Thomas et al. 2015, Davison et al. 2018).

All PHEOs and PGLs are regarded as having malignant potential and thus it is recommended to divide them into metastatic and nonmetastatic instead of malign and benign tumors (Tischler et al. 2017). About 10% of PHEOs and 15–40% of PGLs metastasize (Chrisoulidou et al. 2007, Harari and Inabnet 2011, Choi et al. 2015, Tischler et al. 2017). Metastatic potential of PHEOs and PGLs cannot be interpreted from morphology; thus no scoring system is completely validated today. However, some histological features are associated with metastatic potential, such as high proliferation and necrosis, and risk stratification of these tumors is recommended (Tischler et al. 2017). Major advancement has been achieved in genetics of these tumors and in demonstrating the impact of genetic background on pathogenesis, localization, clinical behavior, and prognosis. According to genetic background, tumors can be divided into three clusters with different pathogenesis (Crona et al. 2017).

The treatment options for metastatic PHEOs and PGLs are limited, but with increasing knowledge of the individual pathogenesis and characteristics of these tumors, possibly new targeted therapies can be developed.

5 Review of the literature

5.1 Adrenal gland and paraganglion system

5.1.1 *Adrenal gland*

The triangular shaped adrenal glands are paired endocrine organs located near the superior poles of the kidneys in the retroperitoneal fat. The glands consist of a yellowish adrenal cortex, which secretes glucocorticoids, mineralocorticoids, and sex steroids, and a reddish-brown medulla, which secretes catecholamines. The cortex and the medulla have different functions, morphology, and embryology (Ross and Pawlina 2006, Mescher 2013). During organogenesis, the intermediate mesoderm gives rise to the adrenal cortex and gonads within the urogenital ridge. At 4 weeks of human gestation an adrenogonadal primordium can be seen. By embryonic week 8, a distinct adrenal primordium separates from the gonadal primordium. Primitive sympathetic cells migrate from the neural crest to form the medulla, which is of neuroectodermal origin. The adrenal gland becomes encapsulated and by the ninth gestational week, a separate organ cranial to the kidney can be seen. The human fetal adrenal cortex has a thick, androgen-producing fetal zone, glucocorticoid-producing definitive zone, and a transitional zone between these two, which is thought to produce cortisol during the third trimester. The fetal zone forms 80–90% of the adrenal cortex during gestation. By birth the adrenal glands weigh 8–9 g each, about twice as much as those of an adult. Postnatally the fetal zone rapidly involutes (Kempna and Fluck 2008, Ross and Louw 2015).

The adrenal glands are surrounded by a connective tissue capsule from which trabeculae with blood vessels and nerves traverse into the adrenal parenchyma. The adrenals get arterial blood from superior, middle and inferior suprarenal arteries, which originate from phrenic and renal arteries and from the aorta. Vessels branch into capsular capillaries and further into fenestrated cortical sinusoidal capillaries supplying adrenocortical cells. Further blood drains into medullary capillary sinusoids. Medullary arterioles pass through cortical trabeculae bringing arterial blood to medullary cells. Thus the medulla has a dual blood supply (see Figure 1). Venules from cortical and medullary sinusoids drain into adrenomedullary collecting veins, which join to form the central adrenomedullary vein. On the right side, it further drains into the inferior vena cava, and on the left side it drains into the left renal vein. The adrenomedullary vein has a tunica media, longitudinally oriented smooth muscle cells, which can contract, decrease the volume of the gland, and enhane the hormone liberation from the medulla into the circulation. In addition, lymphatic vessels are present in the adrenal capsule as well as in the adrenal medulla. Lymphatic vessels probably participate in the delivery of high molecular weight products, like chromogranin A, from the medulla to the circulation (Ross and Pawlina 2006, Mescher 2013).

The medulla contains pale-staining, large chromaffin cells, connective tissue, blood as well as lymphatic vessels, and nerves. The chromaffin cells are organized as clusters and cords and contain the well-developed Golgi apparatus, rough endoplasmic reticulum, and the secretory vesicles, which are 100–300 nm in diameter. The chromaffin cells are divided into two separate types secreting either epinephrine or norepinephrine. Glucocorticoids released from the adrenal cortex induce the enzyme phenylethanolamine-N-methyltransferase, which further causes methylation of norepinephrine to epinephrine (Ross and Pawlina 2006, Mescher 2013, Davison et al. 2018). About 80% of the catecholamines secreted from the medulla are epinephrine. Chromogranins are large soluble proteins binding catecholamines with Ca^{2+} and adenosine triphosphate (ATP) in storage complexes that are released with catecholamines (Ross and Pawlina 2006, Mescher 2013). Chromogranins are used for diagnosing PHEOs and PGLs both biochemically and by immunohistochemistry (IHC).

Chromaffin cells synapse with myelinated presynaptic sympathetic nerve fibers. Nerve impulses cause the release of acetylcholine in presynaptic axons which triggers exocytosis of secretory vesicles in chromaffin cells. The release of catecholamines prepares the body for maximum use of energy and maximum physical effort – the "fight or flight" situation. Axons of medullary ganglion cells reach the cortex and can regulate cortical hormone secretion as well (Ross and Pawlina 2006, Mescher 2013).

The adult adrenal cortex is divided into three zones with different morphology and function (see Figure 1). The outermost zona glomerulosa secretes mineralocorticoids, with aldosterone being the most important. The renin-angiotensin system regulates secretion of mineralocorticoids. The zona fasciculata in the middle secretes mainly glucocorticoids and some weak androgens. The zona reticularis secretes weak androgens, mostly dehydroepiandrosterone (DHEA), its sulfated conjugate (DHEAS), and to some extent also glucocorticoids. Hormonal activity and growth of the inner zones are regulated through the hypothalamic-pituitary-adrenal axis. Corticotrophin-releasing hormone (CRH) from the hypothalamus regulates the secretion of the pituitary adrenocorticotropic hormone (ACTH) which regulates the zona fasciculata and zona reticularis (Ross and Pawlina 2006, Mescher 2013).

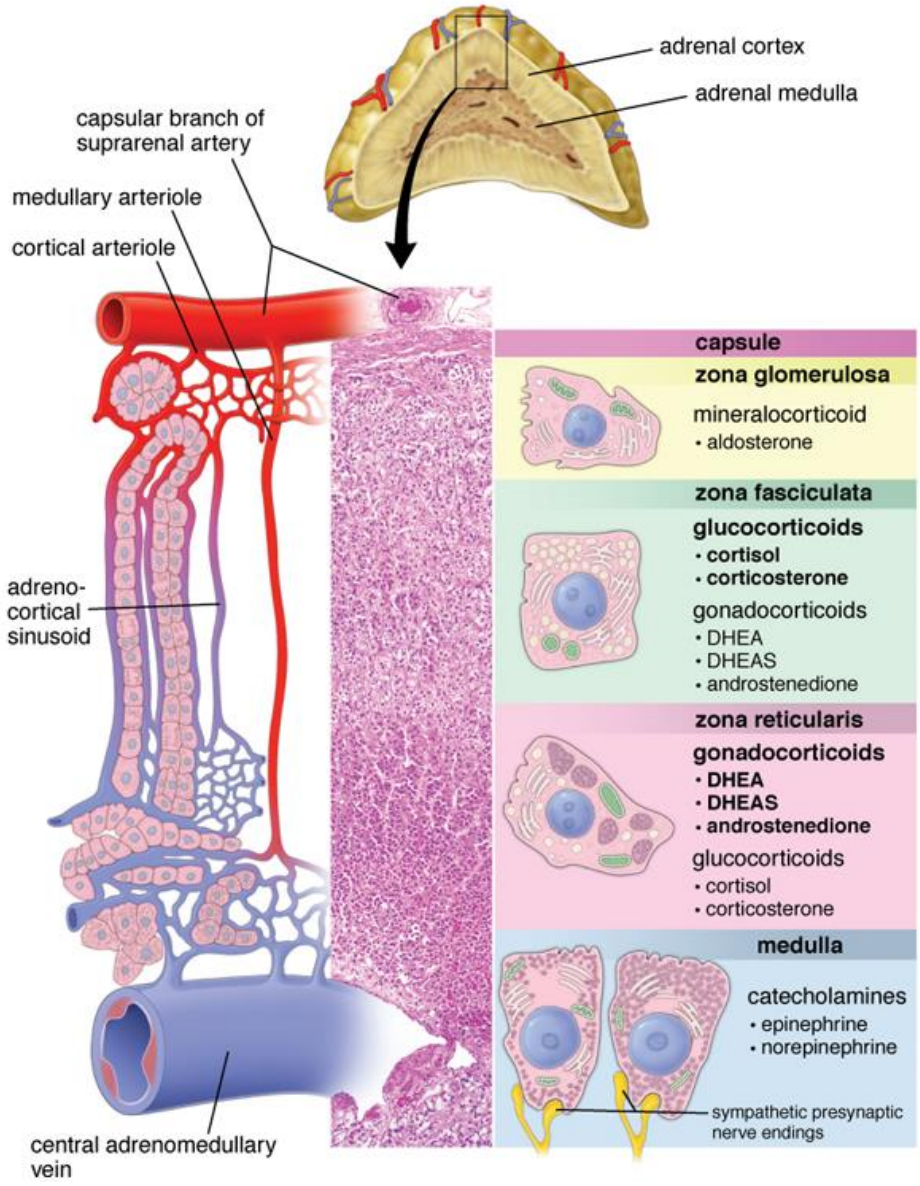

Figure 1. Organization of the cells within the adrenal gland and their relationship to the blood vessels (from Ross and Pawlina 2016).
Reproduced with permission from Wolters Kluwer

5.1.2 *Paraganglion system*

Paraganglia are a neural crest derived groups of cells scattered throughout the body as small masses. The size varies from small microscopic masses up to visible 3 mm clusters. The largest paraganglia are the organ of Zuckerkandl, the aortic sympathetic paraganglia, and intercarotid paraganglia. The paraganglia are either sympathetic or parasympathetic.

Sympathetic paraganglia are located in the adrenal medulla, in prevertebral and paravertebral sympathetic chains, and in the sympathetic nerves, like in the organ of Zuckerkandl, retroperitoneum, thorax, and pelvis (Figure 2A). Sympathetic PGLs can arise in these locations.

Parasympathetic paraganglia are located mainly in the head and neck along the cervicothoracic branches of the glossopharyngeal nerve, along vagal and jugulotympanic nerves where parasympathetic PGL develop (Figure 2B). Some parasympathetic paraganglia like the carotid body paraganglia work as chemoreceptors.

The paraganglia have neuroendocrine chief cells that contain neurosecretory vesicles. The chief cells are arranged into cell nests, which are surrounded by sustentacular cells and rich vasculature (Ross and Pawlina 2006, Love and Anderson 2015, Tischler et al. 2017).

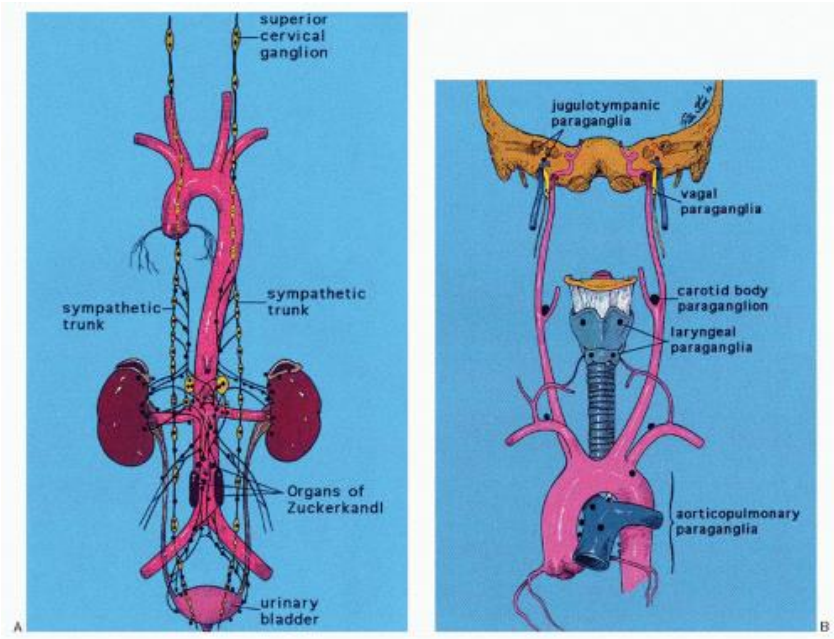

Figure 2A. Anatomical distribution of sympathoadrenal paraganglia.
Figure 2B. Anatomical distribution of paraganglia in head and neck.
(From Lack 2007, p. 283, Fig. 11.1; p. 323, Fig. 12.1.)
Reproduced with permission from American Registry of Pathology

5.2 Pheochromocytomas and paragangliomas

5.2.1 *Epidemiology and risk factors*

Incidence of PHEOs and PGLs ranges from 0.4 to 9.5 cases per one million people per year (Tischler et al. 2017). In Finland about 10–15 PHEOs are diagnosed yearly (Paronen et al. 2013). Sympathetic PGL occur about one tenth as often as PHEOs. The incidence of PHEOs and sympathetic PGLs has been reported to have risen in recent decades (Berends et al. 2018). The increased incidence is associated with a trend of smaller tumor size and higher patient age at diagnosis. The increase in incidence can at least partly be explained by an increased use of imaging studies and biochemical tests for PHEOs and PGLs (Berends et al. 2018).

PHEOs and sympathetic PGLs can occur at any age, but most patients are in their fourth or fifth decades of life. The tumors in children are more often PGLs and are usually hereditary. The incidence is equal in both sexes and the only known risk factor is hereditary background (Tischler et al. 2017). Of patients with hypertension, about 0.2–0.6% have a PHEO (Lenders et al. 2014, Gunawardane and Grossman 2017).

The incidence of head and neck PGLs (HNPGLs) is estimated to be one case per 30,000–100,000 people annually. They represent 20% of all PGLs and 0.6% of head and neck tumors (Tischler et al. 2017). The most common HNPGL is carotid body PGL (57%), the next common being jugular PGL (23%) (Erickson et al. 2001). Some hereditary syndrome is often behind an HNPGL, but also chronic hypoxic conditions such as a high-altitude environment and cyanotic heart disease are thought to predispose to HNPGLs (Tischler et al. 2017).

Of all incidentally found adrenal tumors about 1.5–14% are PHEOs (Davison et al. 2018) and PHEOs are found as incidentalomas in approximately one fourth (Gunawardane and Grossman 2017) to 61% (Baguet et al. 2004, Oshmyansky et al. 2013, Tischler et al. 2017) of cases.

5.2.2 *Genetic basis, pathogenesis, and most important associated syndromes*

Hereditary background is found in about 30–40% of PHEOs and PGLs (Pillai et al. 2016, Crona et al. 2017, Tischler et al. 2017). At least 12 different genetic syndromes and 15 well-characterized driver genes are associated with these tumors. From sporadic PHEOs and PGLs a somatic mutation in genes associated with hereditary PHEO and PGL syndromes can be found in 25–30% of cases. A known germ-line or somatic PHEO/PGL gene mutation can be found in about 60% of tumors (Favier et al. 2015, Pillai et al. 2016).

Different mutations are associated with different pathogenesis. The Cancer Genome Atlas molecular taxonomy nowadays separates PGLs and PHEOs into three main clusters – 1) pseudohypoxic, 2) Wnt signaling, and 3) kinase signaling – according to the underlying mutation and different pathogenesis (Fishbein et al. 2017, Crona et al. 2017). The genotype–phenotype correlations of hereditary PHEOs and PGLs are listed in Table 1.

5.2.2.1 *Pseudohypoxic cluster of pheochromocytomas and paragangliomas*

Hypoxia exists when oxygen concentration is below 21%. In a pseudohypoxic state, cellular oxygen concentration is high enough, but oxygen cannot be processed further due to a distraction in the oxygen-sensing pathways (Jochmanova et al. 2014). Hypoxia and pseudohypoxia activate hypoxia-inducible factors (HIFs), which are transcription factors and are composed of an oxygen-sensitive α subunit and stable β subunit (Jochmanova et al. 2014). Due to the accumulation of oncometabolites and the stabilization of HIFs under normal oxygen pressure, a pseudohypoxic cluster has a pathological hypoxic response.

The pseudohypoxic group can be divided into at least two subgroups: 1) tricarboxylic acid (TCA)-cycle related and 2) *VHL* and *EPAS1/HIF-2α* related. Succinate dehydrogenase (*SDHx*), fumarate hydratase (*FH*), and malate dehydrogenase (*MDH2*) mutations belong to the TCA-cycle related cluster. Mutations in genes encoding these enzymes cause the accumulation of oncometabolites, such as succinate, fumarate and malate, which leads to stabilization of HIF and activation of its target genes. Mutation in *VHL* or *EPAS1* genes leads to stabilization of HIF and activation of HIF target genes, for example those associated with angiogenesis, cell growth, hematopoiesis, and cell migration (Jochmanova et al. 2014, Crona et al. 2017). *EPAS1* mutation activates different genes than *VHL* and *SDHx* and may in the future be a special subgroup (Crona et al. 2017).

5.2.2.2 *Wnt signaling cluster of pheochromocytomas and paragangliomas*

Of sporadic PHEOs and PGLs, 5–10% are thought to arise via the Wnt signaling pathway. Mutations in this group have been found in cold shock domain containing E1 (*CSDE1*) or in gene fusion *UBTF* (upstream binding transcription factor)-*MAML3* (mastermind-like transcriptional coactivator 3) that cause activation of the Wnt and Hedgehog signaling

pathways. These tumors may be more aggressive based on clinical evidence of frequent recurrence and metastasis (Fishbein et al. 2017, Crona et al. 2017).

5.2.2.3 *Kinase signaling cluster of pheochromocytomas and paragangliomas*

The kinase signaling cluster includes mutations that cause abnormal activation of oncogenic kinase signaling pathways like RAS/RAF / extracellular signal-regulated kinase (ERK) and PI3-kinase / protein kinase B (AKT) / mammalian target of rapamycin (mTOR). The most common genes in this group are the *RET* (rearranged during transfection) proto-oncogene and neurofibromin 1 (*NF1*). Also, Myc-associated factor X (*MAX*), transmembrane protein 127 (*TMEM127*), and kinesin family member 1B (*KIF1B*) are included in this group (Pillai et al. 2016). Activation of the *RET* oncogene (gain of function mutation) causes activation of the tyrosine kinase receptor, which leads to activation of the RAS/RAF/ERK and PI 3-kinase/AKT/mTOR pathways. This increases cell proliferation, cell survival, and growth and can lead to development of a PGL or PHEO (Pillai et al. 2016).

5.2.2.4 *Somatic mutations of pheochromocytomas and paragangliomas*

The rate of point mutations in PHEOs and PGLs is low, with a mean of 0.67 per megabase, the mutations becoming more frequent with age (Fishbein et al. 2017, Crona et al. 2017). The frequency of somatic point mutations in PHEOs and PGLs is between that of adrenocortical carcinomas (median 0.9 somatic mutations per Mb) and neuroblastomas (median 0.3 somatic mutations per Mb) (Lawrence et al. 2014, Zheng et al. 2016). The cancers exposed to external mutagens have about a 20-fold higher mutation rate (Lawrence et al. 2014). The burden of somatic mutations seems to be associated with aggressive disease (Fishbein et al. 2017).

Somatic mutations in genes associated with inherited PGL and PHEO have been identified (Luchetti et al. 2015, Pillai et al. 2016, Crona et al. 2017). Chromosomal gains and losses, copy number, and epigenetic changes have been recognized in PHEOs and PGLs. Frequent chromosomal changes are losses of tumor suppressor genes in chromosomes 1p, 3q, gains in 9q, 17q, 19p13.3, 20q and losses in 11p, 11q, 6q, 17p, and 22 (Luchetti et al. 2015, Tischler et al. 2017).

Table 1. Genotype–phenotype correlations of hereditary pheochromocytomas and paragangliomas. (modified from Tischler et al. 2017). Genes 1–11 are grouped in the pseudohypoxic group, and genes 12–17 in the kinase signaling group.

	***Gene* and syndrome**	**Approximate frequency**	**PHEO**	**PGL of abdomen and thorax**	**PGL of head and neck**	**Approximate risk of metastasis**
1	*VHL* VHL	9%	+++	Rare	Very rare	5%
2	*SDHD* PGL 1	5–7%	+	++	++	<5%
3	*SDHSF2* PGL 2	<1%	–	–	++	Low
4	*SDHC* PGL 3	1–2%	Rare	Rare	++	Low
5	*SDHB* PGL 4	6–8%	+	+++	+	30–70%
6	*SDHA* PGL 5	1–2%	Rare	+	+	Low
7	*EPAS1* PZS	Very rare	+	+		29%
8	*EGLN2*	Very rare	+	+		Unknown
9	*EGLN1*	Very rare	+	+		Unknown
10	*FH*	1%	+	+	+	>50%
11	*MDH2*	Very rare		+		Unknown
12	*RET* MEN2	5%	+++	Rare	Very rare	<5%
13	*NF1*	2%	++	Rare	Very rare	12%
14	*TMEM127*	1%	++	+	+	Low
15	*MAX*	1%	+	+	+	10%
16	*KIF1β*	Very rare				Unknown
17	*MEN1*	Very rare	+		+	Unknown

+ occurring, ++ occurring moderately often, +++ occurring often.

5.2.2.5 *Most important associated syndromes*

Familiar paraganglioma syndromes 1–5

SDH is a mitochondrial enzyme containing four subunits: SDHA-D and two assembly factors SDHAF1 and SDHAF2 (Pillai et al. 2016). The SDH enzyme converts succinate to fumarate. In this process two electrons to the electron transport chain are generated. The SDHA and SDHB subunits are located in the mitochondrial matrix. The complex is anchored to the inner mitochondrial membrane by subunits SDHC and SDHD. The SDH mutations cause accumulation of succinate and production of reactive oxygen species. Increased succinate activates hypoxia-sensitive transcription factors and target genes. SDH-deficient PGLs and PHEOs are of methylator phenotype with hypermethylated histones and promoter regions (Tischler et al. 2017).

Mutations in genes encoding subunits of SDH complex II (*SDHA-D* and assembly factor *SDHAF2*) cause familiar paraganglioma-pheochromocytoma syndromes, PGL 1–5, which are autosomal dominant diseases with variable penetrance. These mutations cause the most common form of hereditary PGLs and PHEOs. Different subunit mutations have different genotype–phenotype correlations and different prognosis. Other important *SDH* mutation associated tumors are gastrointestinal stromal tumors, renal cell carcinomas, and pituitary adenomas (Table 2 Benn et al. 2015).

The *SDHB* subunit mutation is the most common, estimated to occur in 6–8% of all PGLs and PHEOs, followed by mutation in the *SDHD* subunit, occurring in 5–6% of these tumors. About half of *SDHB*-mutation associated tumors are extra-adrenal, like abdominal or thoracic PGLs, and they are multifocal in about 10–25% of cases. *SDHD*-mutation associated tumors are mostly HNPGLs and are multifocal in about 60% of cases. *SDHC*-mutation associated PGLs are often solitary HNPGLs (Tischler et al. 2017).

Table 2. Clinical features, associated tumors (penetrance) of PGL syndromes 1–5 (modified from Benn et al. 2015).

Syndrome	*Gene*	PHEO	Thoraco-abdominal PGL	HNPGL	Multifocal	Metastatic	RCC	Other
PGL 1	*SDHD*	~10–25%	20–25%	85%	55–60%	~4%	~8%	GIST and PA
PGL 2	*SDHAF*	0	0	100%	0	0	0	–
PGL 3	*SDHC*	0	Rare	*	15–20%	0	Rare	GIST
PGL 4	*SDHB*	20–25%	50%	20–30%	20–25%	~30%	~14%	GIST and PA
PGL 5	*SDHA*	Rare	Rare	Rare	Rare	Rare	0	GIST and PA

* Lifetime prevalence not yet determined.
GIST = gastrointestinal stromal tumor; HNPGL = head and neck paraganglioma; PA = pituitary adenoma; PHEO = pheochromocytoma; RCC = renal cell carcinoma.

Von Hippel–Lindau syndrome

The autosomal dominant von Hippel–Lindau syndrome (VHL) is caused by a germ-line mutation in the *VHL* gene, which leads to development of different tumors. *VHL* is a tumor suppressor gene and about 20% are *de novo* mutations. The VHL protein is part of the ubiquitin ligase protein complex, which targets HIF1A/HIFα for ubiquitination and proteasomal degradation. When the VHL protein is inactive or in hypoxia, HIF1A and HIF2A stabilize and activate hypoxia-related genes, for example *VEGF* and *cyclinD1*.

Hemangioblastomas in the retina and central nervous system occur in 80% of VHL patients. Other VHL-associated tumors are PHEOs and PGLs, neuroendocrine tumors, renal cell carcinomas, and pancreatic serous cystadenomas. In Finland the incidence of VHL syndrome is 1/53,000 (Orphanet Orpha number ORPHA892). VHL syndrome is divided into different genotype–phenotype correlations. No PHEOs exist in type 1. In type 2A-2B, PHEOs and other tumors are found; in type 2C only PHEOs develop. The PHEOs in VHL syndrome usually secrete norepinephrine and bilateral tumors are common (Martucci and Pacak 2014, Tischler et al. 2017).

Multiple endocrine neoplasia type 2 (MEN2)

The RET protein, which is a receptor tyrosine kinase, regulates cellular proliferation and apoptosis. Activating (gain of function) germ-line mutations in the *RET*-proto-oncogene cause multiple endocrine neoplasia type 2 (MEN2), with an estimated incidence of 1/30,000 (Tischler et al. 2017).

MEN2 has three phenotypes: MEN2A, MEN2B, and familiar medullary thyroid carcinoma (MTC). MEN2A patients represent about 90% of MEN2 cases and have MTC in over 90% of cases, a 50% risk of developing PHEO, and a 15–30% risk of hyperparathyroidism. Patients with rare MEN2B have a 100% risk of developing MTC and a 50% risk of developing PHEO. They also have mucosal ganglioneuromas and marfanoid habitus. Patients with familiar MTC have only an increased risk of this neoplasm. PHEOs in MEN2 usually produce epinephrine, and approximately half of them are bilateral. MEN2-associated PHEOs seldom metastasize (Martucci and Pacak 2014, Tischler et al. 2017).

Neurofibrmatosis type 1

Mutations in the *NF1* gene cause autosomal dominant neurofibromatosis 1 (NF1) syndrome. The product of the *NF* gene is neurofibromin protein, which activates RAS GTPase. Neurofibromin functions as a tumor suppressor and its inactivation leads to increased RAS oncogene signaling (Tischler et al. 2017).

NF1 patients have multiple neurofibromas, freckling of the axilla and/or groin, brain stem gliomas, café au lait spots, PHEOs, duodenal neuroendocrine tumors (NETs), and malignant peripheral nerve sheath tumors. Disease outcome and tumor burden varies (Tischler et al. 2017). The prevalence of NF1 in Finland is about 1/4400 (Poyhonen et al. 2000). About half of the cases are *de novo* mutations. PHEO/PGL are relatively infrequent in NF1. Epinephrine secreting PHEOs are more common than PGLs (Martucci and Pacak 2014). Recently, somatic *NF1* mutation has been associated with sporadic PHEOs (Burnichon et al. 2012).

5.2.3 *Somatostatin receptor expression in pheochromocytomas and paragangliomas*

Somatostatin is a tetradecapeptide that inhibits growth hormone release from the pituitary gland, has an antisecretory effect, and can inhibit proliferation both in normal tissues and in various endocrine tumors (Unger et al. 2008). Somatostatin has also some antiangiogenic effect (Korner 2016).

Somatostatin receptors (SSTR) belong to the G-protein coupled membrane receptors and peptide receptors. In human neoplasias five different SSTR subtypes, SSTR1–5, can manifest in various combinations (Reubi 2003). Like in other NETs, they are all also expressed in PHEOs and PGLs (Reubi 2003, Elston et al. 2015, Kaemmerer et al. 2017).

When somatostatin or its analogs bind to SSTR, the ligand–receptor complex internalizes and activates different intracellular signal transduction cascades (Korner 2016). The antisecretory effect is mediated via a reduction of cyclic adenosine monophosphate (cAMP) and calcium channel activity. Modulation of mitogen-activated protein kinase (MAPK) activity and the activation of phosphotyrosine phosphatases are involved in the antiproliferative effects of SSTRs. Phosphotyrosine phosphatase activation and a decrease in cAMP are brought about by all SSTRs. Different SSTR subtypes have a variable impact on MAPK activity. SSTR4 increases while SSTR3 and SSTR5 decrease MAPK activity. SSTR1 and SSTR2 can both increase and decrease MAPK activity (Vitale et al. 2018). Although receptor internalization is thought to be an important factor for tumor targeting with somatostatin analogs, interestingly even more potent tumor targeting has been achieved with somatostatin antagonists which internalize poorly or not at all (Korner 2016).

In PHEOs and PGLs discordant results regarding SSTR1–5 expression have been published. Similarly, contradictory results of SSTR expression in SDHB-negative tumors have been reported (Mundschenk et al. 2003, Elston et al. 2015, Kaemmerer et al. 2017). In some works, the SSTR2 expression in PHEOs and PGLs has been the most abundant (Elston et al. 2015, Kaemmerer et al. 2017). In other works, SSTR3 has been the most dominant SSTR subtype (Mundschenk et al. 2003, Unger et al. 2008). Variable SSTR1, SSTR4, and SSTR5 positivity has also been reported (Unger et al. 2008, Elston et al. 2015, Kaemmerer et al. 2015).

Octreotide, which has a high affinity for SSTR2 and low affinity for SSTR3 and SSTR5, is the most used somatostatin analog (Korner 2016). Somatostatin analogs have been used to control the hormonal activity of PHEOs and PGLs with variable results (Lamarre-Cliche et al. 2002, Duet et al. 2005, Elston et al. 2015). Radiolabeled somatostatin analogs can be used both in imaging and radiotherapy in PHEOs and PGLs (Gunawardane and Grossman 2017).

5.2.4 *Clinical presentation*

5.2.4.1 *Location of pheochromocytomas and paragangliomas*

The paraganglion system includes the adrenal medulla, where PHEOs originate, and extra-adrenal paraganglia, which can be sympathetic or parasympathetic. Paraganglion originating PGLs are situated in the region of autonomic nervous system ganglia and following nerves. Sympathetic PGLs may be found from the base of the skull to the pelvis along prevertebral and paravertebral sympathetic chains and nerve fibers. Parasympathetic PGLs usually arise in the head and neck along jugular and tympanic nerves and sometimes in the mediastinum along the vagal nerve (Tischler et al. 2017, Crona et al. 2017). The majority of these tumors are intra-adrenal PHEOs, approximately 85–90% (Gunawardane and Grossman 2017, Davison et al. 2018). Of extra-adrenal sympathetic PGLs, most are located below the diaphragm in the para-aortic area, near the adrenals, in the kidney hilus and organ of Zuckerkandl (Tischler et al. 2017). Intrathoracic PGLs constitute around 12% and urine bladder PGLs 10% of sympathetic PGLs. The most common location regarding HNPGLs is the carotid body (57%), followed by jugular (23%) and vagal PGLs (13%) (Tischler et al. 2017). Rare sites for PGLs are, for example, the thyroid (Castelblanco et al. 2012), pancreas (Zhang et al. 2014), mesenterium (Mohd Slim et al. 2015), cauda equina (Sonneland et al. 1986), heart (Wang et al. 2015), and nasopharynx (Said-Al-Naief and Ojha 2008) (Figure 3).

The primary location of a tumor is important because PHEOs and PGLs arising in various locations have different genetic background, different behavior, and different prognosis (Tischler et al. 2017). Sometimes it can be impossible to determine the primary location of the tumor. In the neck region, it can be difficult to separate a cervical sympathetic PGL from a parasympathetic neck PGL. A large infiltrative tumor in the vicinity of the adrenal gland can be either an adrenal PHEO, which infiltrates the surrounding soft tissues, or a PGL arising close to the adrenal gland with infiltration of the gland.

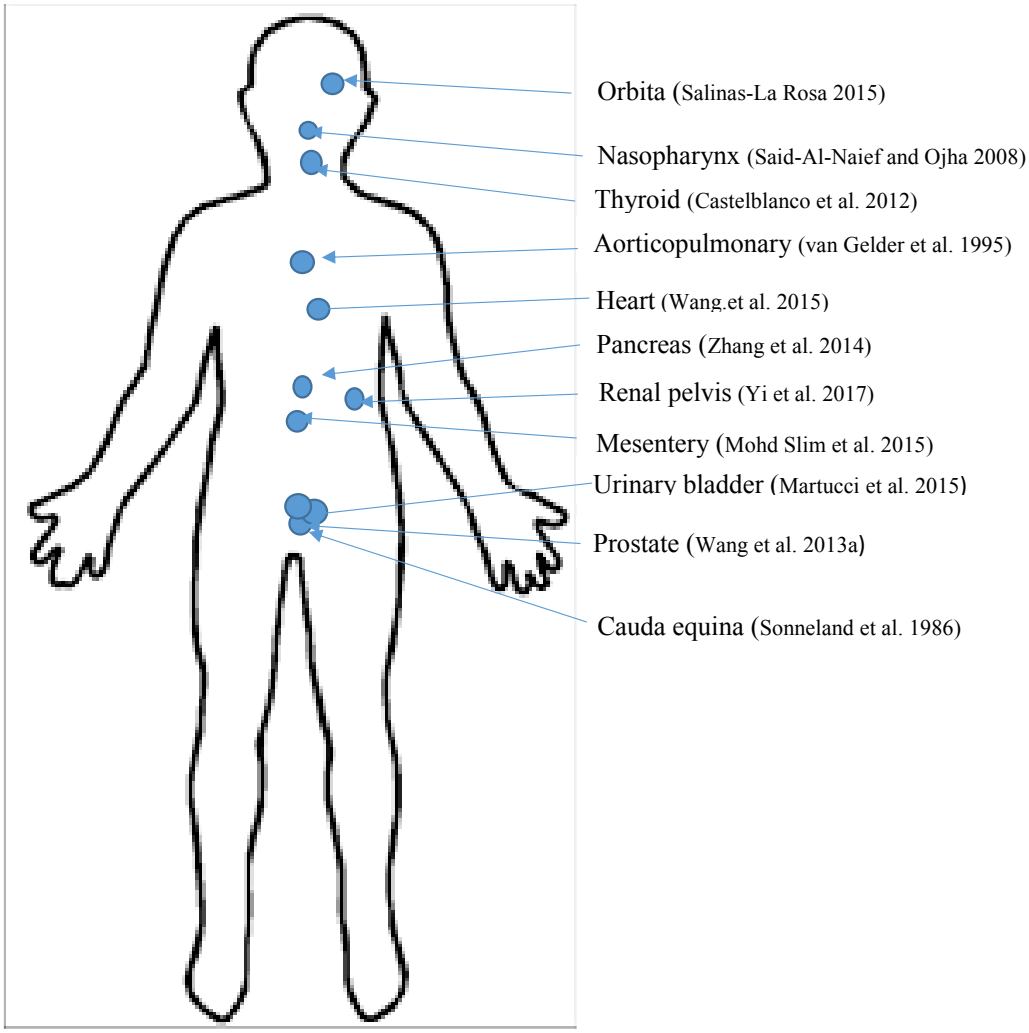

Figure 3. Rare sites of paragangliomas.

5.2.4.2 *Symptoms*

PHEOs and PGLs are called “the great mimickers” because the clinical presentation is very variable and sometimes it can take years from symptoms to diagnosis (Lenders et al. 2014, Thomas et al. 2015, Davison et al. 2018). The amount and quality of hormones secreted by the tumor have an impact on symptoms. Catecholamines act via α-, β-, and dopaminergic receptors. The receptors have different physiological actions and several subtypes (Gunawardane and Grossman 2017). The hormonal activity usually leads to diagnostic investigations because of hormonally-related symptoms, which are usually episodic, so-called “spells,” and are associated with intermittent catecholamine release from the tumor.

Factors that trigger hormone release can be, for example, general anesthesia, drugs, including contrast agents, metoclopramide, and β-adrenergic receptor blockers, trauma to the tumor, exercise, and postural change (Gunawardane and Grossman 2017, Davison et al. 2018). Release of catecholamines can lead to life-threatening crises (Davison et al. 2018) with serious consequences: intracranial hemorrhage, severe arrhythmias, heart failure, and pulmonary edema. Therefore, a nonmetastatic PHEO or hormonally active PGL can also be fatal (Jimenez et al. 2017).

Some PHEOs and PGLs may be asymptomatic. Nonfunctional tumors usually cause symptoms because of the growing tumor size, including pain and nerve paralysis (Tischler et al. 2017, Crona et al. 2017).

Periodic or sustained hypertension is the leading symptom of hormonally active tumors and can be difficult to treat. The classic triad – episodes of palpitation, headache, and profuse sweating – occur in 25–40% of patients (Tischler et al. 2017, Davison et al. 2018). The presence of hypertension with this classic triad should lead thoughts to PHEO or catecholamine-producing PGL.

Other symptoms of PHEOs and PGLs are pallor, anxiety, panic attacks, and abdominal pain (Tischler et al. 2017). The most common symptoms are listed in Table 3. High norepinephrine production can lead to constipation, which occurs in 6% of patients (Thosani et al. 2015). PHEOs can also cause paraneoplastic syndromes like Cushing syndrome caused by the overproduction of ACTH (Nijhoff et al. 2009) and polycythemia due to production of erythropoietin (Pacak et al. 2013). Increased sensitivity of erythropoietin receptors can occur in PHEOs and PGLs with *HIF2A* or *EGLN1/2* mutations (Yang et al. 2015). Also, vasoactive intestinal peptide secretion with watery diarrhea, hypokalemia, and achlorhydria has been described (Tischler et al. 2017).

Table 3. Frequency of signs and symptoms (%) of pheochromocytomas. (modified from Lenders et al. 2005).

Signs and symptoms	**Frequency (%)**
Sustained hypertension	50–60
Paroxysmal hypertension	30
Orthostatic hypotension	10–50
Headache	60–90
Palpitations	50–70
Sweating	55–75
Pallor	40–45
Nausea	20–40
Flushing	10–20
Weight loss	20–40
Tiredness	25–40
Psychological symptoms (anxiety, panic)	20–40
Hyperglycemia	40

5.2.5 *Diagnosis*

Biochemical measurements of catecholamines and their metabolites as well as imaging studies are the basis of diagnosis after clinical suspicion has arisen. Because of the high prevalence of genetic background, genetic consulting and testing is recommended for every PHEO and PGL patient (Lenders et al. 2014).

5.2.5.1 *Biochemical evaluation of pheochromocytomas and paragangliomas*

Indications for biochemical tests are hypertension, especially treatment-resistent hypertension, episodic symptoms referring to catecholamine production, incidental adrenal mass, and known hereditary predisposition to PGL or PHEO (Davison et al. 2018).

Catecholamine production can be demonstrated biochemically from plasma or urine, the plasma test being more convenient. Free metanephrines from plasma or fractionated

metanephrines from urine reflect O-methylation of catecholamines in tumor cells. They are recommended for the initial testing (Lenders et al. 2014). Measuring free metanephrines from plasma together with the dopamine metabolite 3-methoxytyramine gives slightly higher sensitivity (99%) than urinary metanephrines (95%) (Lenders et al. 2014, Lenders and Eisenhofer 2017). Different methods can be used to measure catecholamines and metanephrines, like high-performance liquid chromatography and liquid chromatography / mass spectrometry. Catecholamine values four times above the normal range point strongly toward chromaffin cell originating tumors (Martucci and Pacak 2014).

Most PHEOs produce mainly epinephrine with a varying amount of norepinephrine. Most PGLs secrete predominantly or exclusively norepinephrine (Tischler 2008, Lenders and Eisenhofer 2017). The catecholamine profile can be a clue to genetic syndromes. The dopamine metabolite 3-methoxytyramine either alone or combined with other catecholamine metabolites can point toward SDHB, SDHC, or SDHD mutation. Tumors associated with MEN2 or NF1 usually produce epinephrine, with high levels of metanephrine in plasma or urine. In VHL syndrome, isolated norepinephrine and normetaepinephrine production can be detected (Eisenhofer et al. 2011, Eisenhofer and Peitzsch 2014, Tischler et al. 2017).

Chromogranin A, a polypeptide secreted by chromaffin cells, is elevated in plasma in 91% of PHEO/PGL patients. It is also elevated in other neuroendocrine tumors and even in neuroendocrine hyperplasias. It is thus not specific to PHEOs and PGLs, but it can be valuable in the follow-up. By combining catecholamine measurement with chromogranin A, a very high diagnostic sensitivity is possible (Grossrubatscher et al. 2006, Martucci and Pacak 2014).

5.2.5.2 *Imaging studies*

An important part of diagnosis is imaging. Anatomical location or functional status, giving information of possible treatment options, can be estimated. Examples of imaging methods used are ^{123}I-metaiodobenzylguanidine (MIBG) scintigraphy or somatostatin analog positron emission tomography (PET) computed tomography (CT).

Computed tomography

CT is a sensitive first line imaging modality when a tumor is suspected (Lenders et al. 2014). PHEOs and PGLs have variable appearance at CT. They usually have a rich capillary network, can be solid or cystic, heterogenous or more homogenous, and with or without calcifications (Gunawardane and Grossman 2017). Most PHEOs have Hounsfield units (HUs) over 10 (Blake et al. 2004, Davison et al. 2018). In contrast washout evaluation, these tumors have variable patterns, the majority of PHEOs having a delayed washout (Blake et al. 2004). With the increasing use of CT, PHEOs and PGLs can also be found as incidentalomas.

Magnetic resonance imaging

Magnetic resonance imaging (MRI) is useful in the localization of tumors, especially with HNPGLs and rare intracardial PGLs. MRI is also informative in metastatic disease (Lenders et al. 2014, Lenders and Eisenhofer 2017). Most tumors have a high signal intensity at T2-weighted imaging and low signal intensity at T1-weighted imaging (Gunawardane and Grossman 2017). MRI is the preferred imaging method due to the lack of radiation exposure especially in children and pregnant women, and in the follow-up of SDHx mutation carriers (Lenders et al. 2014, Gunawardane and Grossman 2017).

Metaiodobenzylguanidine scintigraphy

The radiopharmaceutical agent MIBG is an analog of noradrenaline and accumulates mostly in catecholamine-producing cells and in electron-dense catecholamine storing granules. MIBG imaging can be used for confirmation of diagnosis of adrenal lesions, to search for metastasis of PHEOs and PGLs, and for estimation of suitability of MIBG therapy. Tissues innervated by the sympathetic system, for example the heart and salivary glands, take up MIBG.

^{123}I-labeled MIBG can be visualized with single-photon emission computed tomography (SPECT) or SPECT combined with CT (SPECT-CT). ^{123}I-labeled MIBG has a specificity of 70–100% for PHEOs and 84–100% for PGLs, and a sensitivity of 85–88% for PHEOs and 56–75% for PGLs (Gunawardane and Grossman 2017, Davison et al. 2018). Because of the low sensitivity (less than 50%) for metastatic PGLs and especially for SDHB-related PGLs, other imaging modalities are recommended for these tumors, except if iodine-131 (^{131}I) MIBG based therapy is planned (Lenders et al. 2014). Some drugs can interfere with MIBG scanning, for example tricyclic antidepressants, labetalol, and sympathomimetics. Also, strong physiological uptake or small tumor size can interfere with image interpretation (Gunawardane and Grossman 2017, Davison et al. 2018).

Somatostatin analog positron emission tomography computed tomography

Because the majority of PHEOs and PGLs express somatostatin receptors, labeled somatostatin analogs can be used for imaging PHEOs and PGLs, visualized with PET combined with CT (PET-CT) (Davison et al. 2018). The octapeptide octreotide or its modifications are used as ligands, which are fused to chelators and labeled with various radiometals (Ambrosini et al. 2011). Instead of the traditional octreotide scintigraphy, more sensitive DOTANOC/DOTATATE ligands are increasingly used (Davison et al. 2018). DOTANOC has a high affinity for SSTR2, 3, and 5 (Ambrosini et al. 2011). ^{68}Ga-DOTANOC PET-CT has good accuracy for both SDHx-related and sporadic metastatic PHEOs and PGLs. It is also useful for the imaging of HNPGLs (Lenders and Eisenhofer 2017, Davison et al. 2018). Because same ligands used in imaging can be used also in peptide receptor radionuclide therapy (PRRT), SSTR imaging is important when estimating patient suitability for possible PRRT therapy.

FDG positron emission tomography computed tomography

PET with 2-deoxy-2-[fluorine-18] fluoro-D-glucose (^{18}F-FDG), which is an analog of glucose, visualizes cancer cells based on their increased glucose uptake and glycolysis and indicates metabolic abnormalities before morphological alterations occur. ^{18}F-FDG PET/CT combines simultaneous PET and CT data and gives an exact anatomical localization of the ^{18}F-FDG PET positive lesions (Almuhaideb et al. 2011). ^{18}F-FDG PET is sensitive in metastatic PGLs and PHEOs, especially in SDHB-related disease (Timmers et al. 2007, Lenders et al. 2014).

5.2.6 *Treatment*

5.2.6.1 *Preoperative and surgical treatment*

Surgery is the only curative treatment for PHEOs and PGLs. With good preoperative medical preparation, modern anesthesia, and surgical techniques, perioperative mortality rates are low at less than 1% (Lenders and Eisenhofer 2017). However, operation of a catecholamine-producing tumor is a high-risk procedure and a multidisciplinary team including different specialist experienced surgeons, endocrinologists, and anesthesiologists should treat these patients (Gunawardane and Grossman 2017).

Preoperative treatment

Adequate preoperative medication is necessary to make the operation safe. The purpose of this is to prevent dangerous complications due to massive bouts of catecholamine being released from the tumor. These preparations are recommended even for normotensive, asymptomatic patients (Lenders et al. 2014, Gunawardane and Grossman 2017, Lenders and Eisenhofer 2017). PHEO/PGL patients should always go through a proper cardiovascular evaluation to rule out possible left ventricular, even subclinical, failure (Lenders and Eisenhofer 2017). To achieve effective α blockage, most centers use a noncompetitive α-adrenoceptor blocker from one to two weeks before operation. Calcium channel blockers can also be used in addition. After proper α-adrenoceptor blockage, β-adrenoceptor blockage can be used to control tachycardia and tachyarrhythmias. Before and during operation, sufficient liquid balance should be guaranteed (Lenders et al. 2014, Gunawardane and Grossman 2017, Lenders and Eisenhofer 2017, Davison et al. 2018).

Surgical treatment

In patients with a PHEO, the standard surgical technique in operation is laparoscopic, minimally invasive removal of the adrenal gland by either a posterior retroperitoneal or transperitoneal approach (Barczynski et al. 2014, Gunawardane and Grossman 2017). For large (over 6 cm) or invasive PHEOs, an open resection is recommended to assure complete

tumor resection and to avoid tumor rupture leading to local recurrences (Lenders et al. 2014). Operation techniques for PGLs depend on the location and tumor size (Lenders and Eisenhofer 2017). Partial adrenalectomy could be the preferred option in patients with hereditary tumor to avoid lifelong steroid replacement therapy (Lenders et al. 2014, Castinetti et al. 2016).

5.2.6.2 *Radiation therapy*

Besides radionuclide therapies – ^{131}I-MIBG and PRRT – direct external irradiation can be given as palliative treatment, for example for bone metastases. Radio-frequency ablation has been used for liver and bone metastases (Martucci and Pacak 2014).

Metaiodobenzylguanidine

^{131}I-MIBG has been used as palliative treatment since the 1980s for metastatic PHEOs. Tumors that are positive in imaging with ^{123}I-MIBG can be treated with ^{131}I-MIBG. Labeled MIBG is transported into tumor cells. Emitted β radiation causes radiation-induced cell death (Castellani et al. 2010, Jimenez et al. 2017, Roman-Gonzalez and Jimenez 2017, Davison et al. 2018). ^{131}I-MIBG can be given as multiple relatively low doses or as a limited number of high doses. Soft tissue metastases respond better than bone metastases. Adverse effects, which are usually dose dependent, are seen in 47–54% of patients receiving MIBG therapy. These adverse effects include anorexia, nausea, vomiting, hypothyroidism, ovarian failure, leukopenia, and thrombocytopenia (Castellani et al. 2010, Jimenez et al. 2017, Davison et al. 2018).

Ultratrace iobenguane I-131, a new radiopharmaceutical agent which contains no unlabeled MIBG and has high specificity, is a promising improvement in the MIBG treatment options (Roman-Gonzalez and Jimenez 2017).

Peptide receptor radionuclide therapy

Peptide analogs having affinity for SSTRs can be coupled with a suitable radioisotope, for example lutetium-177 (^{177}Lu) or yttrium-90 (^{90}Y), to give targeted peptide receptor radionucleotide therapy (PRRT) to patients with SSTR-positive tumors at imaging (Korner 2016). Only a few reports on PRRT treatment for metastatic PHEOs or PGLs have been published, but results are promising. Nastos et al. (2017) studied 22 patients who had progressive or metastatic PGL or PHEO. Of 30 treatments two were with ^{177}Lu DOTATATE, 12 with ^{90}Y-DOTATATE, and 16 with ^{131}I-MIBG. PRRT-treated patients had significantly increased progression-free survival and response to treatment compared with ^{131}I-MIBG treated patients. For overall survival, no difference was found. In comparison of

only patients with PGLs, overall survival, progression-free survival, event-free survival, and response to treatment were significantly better in the PRRT-treated group than in the ^{131}I-MIBG treated group (Nastos et al. 2017).

Radionuclide treatment is less toxic than conventional cytotoxic agents. It reduces hormonal secretion by the tumor (Gunawardane and Grossman 2017). However, severe adverse reactions have been described in association with PRRT therapy for PGLs and PHEOs, including catecholamine crisis and tumor lysis syndrome (Makis et al. 2015).

5.2.6.3 *Medical treatment*

Cytotoxic treatment

Chemotherapy is given as palliative treatment for metastatic PHEOs and PGLs. The most common chemotherapy combination, used since 1985, is cyclophosphamide, vincristine, and dacarbazine (Roman-Gonzalez and Jimenez 2017). Chemotherapy may relieve symptoms, slow down tumor growth, and even shrink the tumor (Martucci and Pacak 2014). Niemeijer et al. (2014) reported partial response in tumor volume in about 37% of patients and partial response in catecholamine secretion in about 40% of patients, but the authors could not exclude overestimation of response, because some initiations of treatments were poorly described in the studies included in this review (Niemeijer et al. 2014).

About 50% of patients with newly diagnosed metastatic PHEO or PGL, who were treatment naive, had minimal or no progression of disease one year after diagnosis. They had no symptoms of tumor burden, and catecholamine excess could easily be controlled with medication (Hescot et al. 2013). Thus, patients most likely to benefit from chemotherapy are those with rapidly progressing tumor burden, those with bone metastases, and those with severe symptoms because of catecholamine excess (Jimenez et al. 2017).

New targeted medicines and future medicines

Large studies on the use of somatostatin analogs in PHEOs and PGLs are lacking. Lamarre-Cliche et al. carried out a prospective study including 10 patients with metastatic or recurrent PHEO treated with slow-release octreotide three times in an interval of one month. They found no significant difference in symptoms, blood pressure, metanephrine excretion, plasma catecholamine, or chromogranin A concentrations measured one month after the third injection (Lamarre-Cliche et al. 2002). Duet et al. gave three doses of long-acting somatostatin analog to eight patients with 18 HNPGLs every 28 days and measured tumor size one month after the third injection. The average shrinkage in HNPGLs was 4.0±10.0%. Of the 18 PGLs, only two shrank more than 20% (Duet et al. 2005). However, new long-

acting somatostatin analogs are being developed with affinity to more than one SSTR subtype.

Many multi-tyrosine kinase inhibitors have been studied in the treatment of metastatic PGLs and PHEOs, for example sunitinib, axitinib, pazopanib, and cabozantinib, which all inhibit angiogenesis (Jimenez et al. 2017, Roman-Gonzalez and Jimenez 2017). Some metastatic PHEOs and PGLs use a hypoxia–pseudohypoxia environment to grow and survive. This environment may keep the immune system from recognizing neoplastic cells and have a tumor-promoting effect by immunosuppression. The immune checkpoint receptor, programmed cell death protein 1 (PD-1), prevents immune attack on tissues. Many cancers are capable of producing proteins that activate PD-1 receptors. Pembrolizumab is an antibody that blocks the PD-1 receptor in the lymphocytes and helps the immune system to attack neoplastic cells. Studies where metastatic PGL and PHEO patients are treated with pembrolizumab are currently ongoing (Roman-Gonzalez and Jimenez 2017). Temozolomide, an oral alternative to dacarbazine, was a promising treatment alternative for patients with SDHB mutation associated metastatic PGLs and PHEOs in a study by Hadoux et al. (2014) which included 15 patients, but another paper could not confirm this result (Ayala-Ramirez et al. 2012). SDHB-mutated tumors have O-methylguanine-DNA methyltransferase (MGMT) promoter hypermethylation. Silencing of MGMT expression can explain the action of temozolomide (Hadoux et al. 2014).

5.2.7 *Gross appearance and histopathology*

Tumor morphology can often predict outcome. However, in PHEOs and PGLs histopathology is a poor predictor of prognosis. Many different scoring systems have been proposed for PHEOs and PGLs, but none of them is completely validated or accepted.

Macroscopy
PHEOs and PGLs are usually 2–6 cm in diameter, but some tumors may be over 10 cm. Tumor color can be gray-pink, violet, or tan when fresh tissue is seen and often yellow after formalin fixation (Figure 4). Hemorrhage, degenerative changes, and cystic change are common (Tischler et al. 2017).

Histopathology
Wide variation of cytological features and architecture can be seen in PHEOs and PGLs. The tumors are composed of polygonal chief cells, which can be reminiscent of normal chromaffin cells of the adrenal medulla. Tumor cells may have granular, pale, or basophilic cytoplasm. Nuclear and cellular pleomorphism are often seen, and the cell size varies a lot (Figure 4). Spindle tumor cells and intracytoplasmic hyaline globules can be sometimes found. PHEOs and sympathetic PGLs have a similar morphology. Parasympathetic PGLs may be more cellular than sympathetic PGLs (Tischler et al. 2017).

Growth pattern can appear as the classic cell nests “Zellballen”. Also, diffuse or trabecular growth or even large confluent nests can be found. A second cell population is called sustentacular cells and can be demonstrated at the periphery of the chief cell nests or scattered between chief cells. These cells can be visualized by immunohistochemical staining for S-100 protein and glial fibrillary acidic protein (GFAP). The proportion of sustentacular cells varies and a lack of these cells has been associated with more aggressive tumors (Tischler 2008, Feng et al. 2009).

Fibrous bands and a rich vascular network are found between tumor cells. Tumors have often hemorrhage and hemosiderin deposits. Also, composite tumors having components of neurogenic tumors such as ganglioneuroma, ganglioneuroblastoma, neuroblastoma, or peripheral nerve sheath tumor, and PHEOs exist (Tischler et al. 2017).

Although no histological scoring system can unequivocally predict the metastatic potential of a tumor, some histological features are associated more often with metastatic disease, and thus a risk stratification for tumors is recommended. Features associated with metastatic PHEOs and PGLs include five broader categories: 1) invasive growth (periadrenal and surrounding soft tissue, vascular or capsular invasion), 2) cytological features (spindle cells, cellular monotony, small cells, high cell density, extreme pleomorphism), 3) necrosis, 4) proliferation (increased Ki-67 index, increased amount of mitoses or atypical mitoses), and 5) architectural variation (diffuse growth, enlarged confluent cell nests) (Tischler et al. 2017).

The two most acknowledged scoring systems are Thompson’s Pheochromocytoma of the Adrenal Gland Scaled Score (PASS) (Thompson 2002) and Grading of Adrenal Pheochromocytoma and Paraganglioma (GAPP) (Kimura et al. 2014a, b). The PASS score has only histological features and is valid only for PHEOs. Tumors with a PASS score ≥4 can behave more aggressively. The GAPP score includes histological parameters, an immunohistochemical Ki-67 index, as well as hormonal activity of the tumor. According to the score, tumors are divided into three risk categories: well-differentiated (0–2 points), moderately differentiated (3–6 points), and poorly differentiated (7–10 points), with different survival and risk of metastases.

Salmenkivi et al. scored histologically 105 PHEOs and PGLs. All metastatic tumors had at least one histologically suspicious feature: >5 mitoses/10 high power field (HPF), necrosis, and capsular or vascular invasion. Tumors with histologically suspicious features but without metastases were called borderline tumors (Salmenkivi et al. 2003a). These different scoring systems include common features. They are presented in Table 4, where similar features are pinpointed by color.

Table 4. Pheochromocytoma of the Adrenal Gland Scaled Score (PASS) (Thompson 2002) on the left, grading of Adrenal Pheochromocytoma and Paraganglioma (GAPP) score (Kimura et al. 2014a) on the right, and Salmenkivi score below (Salmenkivi et al. 2003a). For scoring systems, common parameters are highlighted in the same color.

PASS score	
Histomorphological parameter	**Score**
Nuclear hyperchromasia	1
Profound nuclear pleomorphism	1
Capsular invasion	1
Vascular invasion	1
Extension into periadrenal adipose tissue	2
Atypical mitotic figures	2
Greater than 3 mitotic figures / 10HPF	2
Tumor cell spindling	2
Cellular monotony	2
High cellularity	2
Central or confluent tumor necrosis	2
Large nests or diffuse growth (>10% of tumor volume)	2
Total maximum score	**20**

HPF = high power field.

GAPP score	
Parameters	**Points scored**
Histological pattern	
Zellballen	0
Large and irregular cell nests	1
Pseudorosette (even focal)	1
Cellularity	
Low (<150 cells/U)*	0
Moderate (150–250 cells/U)	1
High (more than 250 cells/U)	2
Comedo necrosis	
Absence	0
Presence	2
Vascular or capsular invasion	
Absence	0
Presence	1
Ki-67 labeling index	
<1	0
1–3	1
>3	2
Catecholamine type	
Epinephrine type (E or E+NE)	0
Norepinephrine type (NE or NE+DA)	1
Nonfunctioning type	0
Total maximum score	**10**

* U: area of grid of 10×10 mm, on eyepiece under 400× microsope.

Salmenkivi score
Histologically suspicious features
Necrosis
Vascular invasion
Capsular invasion
Mitosis >5/10 HPF

5.2.8 *Immunohistochemistry and differential diagnosis*

IHC is an important tool in confirming the diagnosis of PHEO or PGL and in differential diagnosis (Table 5). PHEOs and most PGLs are strongly positive at chromogranin A staining, but some HNPGLs can have weak or even negative chromogranin A staining. PHEOs and PGLs express also other neuroendocrine markers such as synaptophysin, CD56, and neuron-specific enolase (NSE). Cytokeratins are negative, with the exception of some parasympathetic PGLs like filum terminale PGL that have been reported to express cytokeratin (DeLellis et al. 2004). Sustentacular cells express S-100 and/or GFAP (Tischler et al. 2017). PHEOs and PGLs have variable SSTR1–5 positivity (Elston et al. 2015).

SDHB IHC is a good method for screening possible genetic background of PGLs and PHEOs. All SDHx mutations result in the loss of SDHB protein, which can be shown immunohistochemically as SDHB-negative staining (Figure 4). In addition, a SDHA antibody is available, staining being negative in SDHA-mutated tumors (Papathomas et al. 2015).

Table 5. Immunohistochemical differential diagnosis of pheochromocytomas (PHEOs) and paragangliomas (PGLs).

Neoplasia or metastasis	**Chrom A**	**Synapto physin**	**Cytokera tins**	**MART1 MelanA**	**Inhibin α**	**Calcito nin**	**CEA**	**CD45**
PHEO or PGL	+	+	−	−	−	−	−	−
Adrenal cortical neoplasia	−	+/−	+/−	+	+/−	−	−	−
Neuroendocrine tumor	+	+	+	−	−	−	+/−	−
Renal cell carcinoma	−	−	+	−	−	−	−	−
Urothelial carcinoma	−	−	+	−	−	−	−/+	−
Hepatocellular carcinoma	−	−	+	−	−	−	+	−
Adenocarcinoma	−	−	+	−	−	−	+/−	−
Melanoma	−	−	−	+	−	−	−	−
Lymphoma	−	−	−	−	−	−	−	+
Medullary thyroid carcinoma	+	+	+	−	−	+	+/−	−

CEA = carcinoembryonic antigen.
+ positive, +/− mostly positive, −/+ mostly negative, − negative.

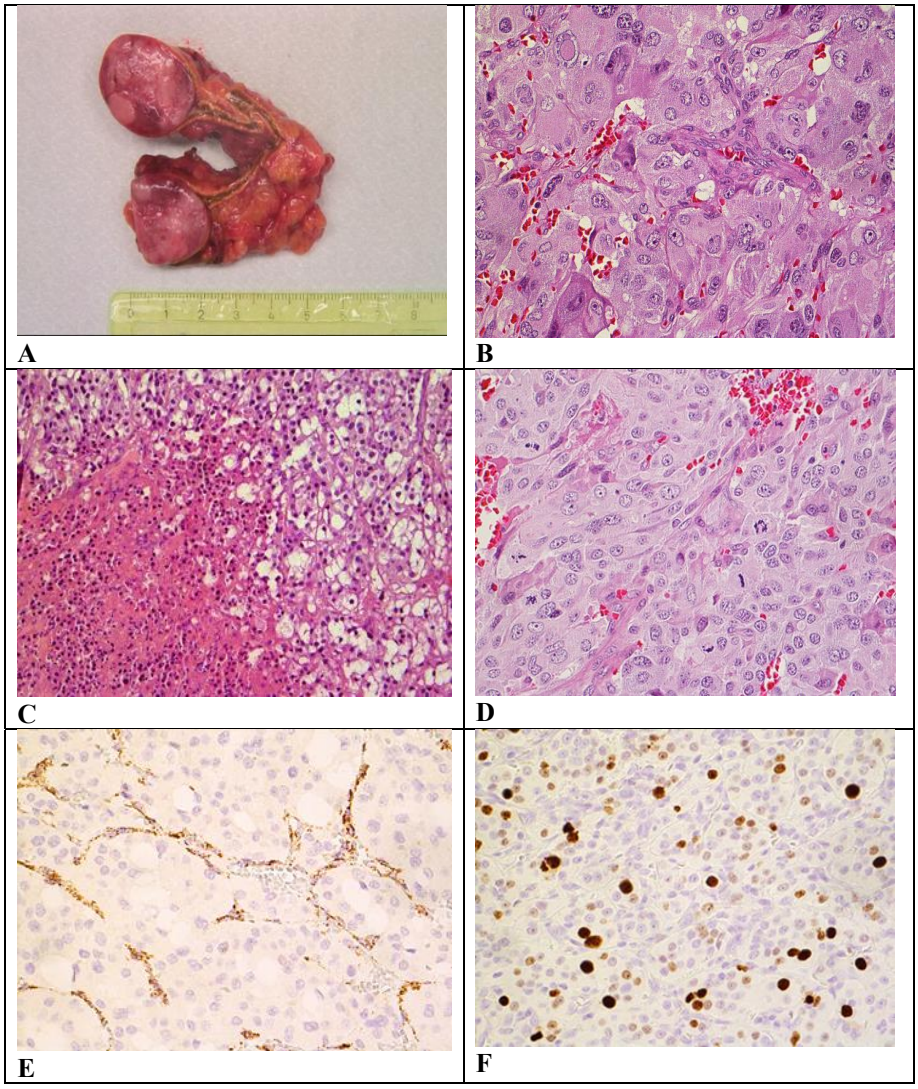

Figure 4 A) A nonmetastatic PHEO in adrenal medulla. B) Variable nuclear size and basophilic cytoplasm in a metastatic PHEO. C) Tumor necrosis in a metastatic PHEO. D) Mitoses in a metastatic PHEO E) SDHB-deficient tumor cells in IHC. Endothelial cells stain positively as an internal control. F) High Ki-67 index in a PGL.

5.2.9 *Metastatic pheochromocytomas and paragangliomas and factors associated with metastatic potential*

All PHEOs and PGLs are considered to have a varying degree of metastatic potential. It is more accurate to call these tumors nonmetastatic and metastatic rather than benign and malignant (Tischler et al. 2017). About 15–40% of PGLs and 10% of PHEOs metastasize (Harari and Inabnet 2011, Choi et al. 2015, Tischler et al. 2017). The diagnosis of metastatic disease should be done with caution as metastases should be found at a site where paraganglionic tissue is not normally present to exclude the possibility of multiple primary tumors. In particular, patients carrying a susceptibility gene mutation can have multiple primary tumors. About 50% of patients with metastatic PHEOs and PGLs develop metastases metachronously. It can take years or even decades after initial diagnosis for metastases to appear (Ayala-Ramirez et al. 2011, Ayala-Ramirez et al. 2013). The most common locations for metastases are the lymph nodes (80%), skeleton (72%), lungs (50%), and liver (50%) (Jimenez et al. 2017).

Up to 34–60% of patients with metastatic disease are alive after 5 years from discovery of metastases (Tischler et al. 2017). Thus, progression of metastatic disease is variable and difficult to predict. Some patients can have indolent disease with a good quality of life for several years, while others have aggressive fast spreading disease with poor response to treatment (Jimenez et al. 2017). Liver and lung metastases are associated with shorter survival than bone metastases (Ayala-Ramirez et al. 2013). In addition, SDHB mutation associated metastatic disease has a worse prognosis (Blank et al. 2010, Martucci and Pacak 2014, Tischler et al. 2017).

In a study by Zelinka et al. (2011), age at diagnosis was an independent risk factor regardless of genetic background. The mean age for patients with metastatic disease was 41.4 years and that of nonmetastatic disease 50.2 years. Dhir et al. (2017) studied 157 PHEOs/PGLs (44 malignant, 113 benign). Patients with metastatic disease were younger – median 42 years versus 50 years. In multivariable analysis, younger age was associated with malignancy (Dhir et al. 2017).

Tumor location is a prognostic factor. PGLs metastasize more often than PHEOs. PGLs with highest metastatic rate are located under the diaphragm in the para-aortic area, in the organ of Zuckerkandl, and in the mediastinum (Ayala-Ramirez et al. 2011). Of vagal PGLs, approximately 16% metastasize, whereas metastases in all HNPGLs are found only in about 4–6% of cases (Tischler et al. 2017).

The size of the primary tumor predicts the outcome of both PHEOs and PGLs. In a study by Eisenhofer et al., primary metastatic tumors were 3.6-fold larger in volume than nonmetastatic PHEOs and PGLs. The mean tumor size for metastatic tumors was 7.2 cm and for nonmetastatic tumors 4.7 cm (Eisenhofer et al. 2012). Ayala-Ramirez et al. (2011) studied the size of PHEOs and PGLs of 290 patients, 89 having a metastatic disease and 201 a nonmetastatic disease. The median tumor size was 8.2 cm for metastatic tumors and 4.9 cm for nonmetastatic tumors ($P<0.0001$). However, 16% of metastatic tumors were smaller than 5 cm, the majority of these being PGLs (78.6%). Also, in a study by de Wailly et al., metastatic PHEOs were significantly larger than nonmetastatic PHEOs (de Wailly et al. 2012). The median survival time for patients with tumors 5 cm or larger was shorter than for those with smaller tumors (Ayala-Ramirez et al. 2011).

In multivariate analysis, location was a more powerful predictor of metastases than size. For the TNM staging of PHEOs and PGLs, a cutoff value of 5 cm was chosen between classes T1 and T2 (Table 6). Functional sympathetic PGLs of any size are T2 tumors.

Table 6. TNM staging of tumors of the adrenal medulla and extra-adrenal paraganglia (Roman-Gonzalez and Jimenez 2017).

Primary tumor size			
TX	Primary tumor cannot be assessed		
T1	Tumor <5 cm in greatest dimension, no extra-adrenal invasion		
T2	Tumor ≥5 cm or sympathetic paraganglioma of any size, no extra-adrenal invasion		
T3	Tumor of any size with invasion into surrounding tissues (e.g., liver, pancreas, spleen, and kidneys)		
Regional lymph nodes			
NX	Regional lymph nodes cannot be assessed		
NO	No lymph node metastasis		
N1	Regional lymph node metastasis		
Distant metastasis			
M0	No distant metastasis		
M1	Distant metastasis		
	M1a: distant metastasis to only bone		
	M1b: distant metastasis to only distant lymph nodes/liver or lung		
	M1c: distant metastasis to bone and multiple other sites		
Stage grouping			
Stage 1	T1	N0	M0
Stage 2	T2	N0	M0
Stage 3	T1	N1	M0
	T2	N1	M0
	T3	Any N	M0
Stage 4	Any T	Any N	M1

Hormonal activity of the tumor can give a clue to the metastatic potential of a PHEO or PGL. Catecholamine synthesis in poorly differentiated tumors can be incomplete, leading to deficient production of noradrenaline. Therefore, metastatic tumors can produce high levels of dopamine and its metabolites. In particular, elevated levels of 3-methoxytyramine may be associated with metastatic disease (Eisenhofer et al. 2012, Gunawardane and Grossman 2017, Lenders and Eisenhofer 2017). Also, very high serum chromogranin A levels have been associated more often with metastatic disease (Gunawardane and Grossman 2017). Metastatic tumors also produce more often noradrenaline (Zelinka et al. 2011).

Tumors with different genetic background have different metastatic potential. SDHB germ-line mutation is one of the strongest factors predicting metastatic disease (Baysal and Maher 2015). *SDHB* mutation leads to activation of HIFs, which have over 100 target genes regulating many neoplasia-associated functions like angiogenesis, invasion, metastasis, cell

death, cancer stem cell maintenance, and proliferation. However, activation of HIF-dependent genes does not explain the metastatic potential alone because other SDHx-mutated tumors are less aggressive. One explanation could be that the hypermethylation phenotype, associated with SDHB-mutated PHEOs and PGLs, would abnormally activate the epithelial-mesenchymal transition (Letouze et al. 2013, Loriot et al. 2012, Roman-Gonzalez and Jimenez 2017).

Germ-line mutations in the *FH* gene (Castro-Vega et al. 2014) and *EPAS1/HIF2A* gene (Tischler et al. 2017) are associated with an aggressive disease. Wnt signaling tumors, which are sporadic tumors, and tumors having *UBTF-MAML3* gene fusion or *CSDE1* mutation are also thought to be aggressive. The burden of somatic mutations seems to be associated with aggressive PHEOs and PGLs (Fishbein et al. 2017). Somatic *NF1* and *ATRX* mutations have been associated with metastatic potential (Burnichon et al. 2012, Fishbein and Nathanson 2017). *VHL*- and *RET*-associated PHEOs metastasize in less than 5% of cases (Gunawardane and Grossman 2017).

The proliferation index of Ki-67 IHC is frequently used to estimate the aggressiveness of many different neoplasias. High Ki-67 index has been reported in metastatic PHEOs and PGLs as well. De Wailly et al. studied 53 PHEOs with seven metastatic cases. Metastatic PHEOs had significantly higher Ki-67 values, and high Ki-67 also correlated with tumor necrosis. All metastatic tumors had Ki-67 >4%, but one nonmetastatic PHEO had a Ki-67 of 11% (de Wailly et al. 2012). In a study of 43 tumors by August et al., 85% of tumors with MIB1/Ki-67 over 5% metastasized (August et al. 2004). Also in other studies, a relationship between high Ki-67 index and aggressive behavior of PHEOs and PGLs has been shown (Tavangar et al. 2010b). However, metastatic tumors with low Ki-67 index exist and some nonmetastatic tumors show relatively high proliferation, so Ki-67 has only a limited value as a single prognostic parameter.

Other markers associated with metastatic potential of pheochromocytomas and paragangliomas

Because histology gives us scant information of the prognosis of PHEOs and PGLs, a lot of studies have tried to find biomarkers associated with the metastatic potential of these tumors (Table 7). No single marker unequivocally indicates the risk of metastases.

Table 7. Biomarkers associated with metastatic potential of pheochromocytomas (PHEOs) and paragangliomas (PGLs).

Biomarker	**Expression in metastatic PHEOs and PGLs**	**Reference**
Human telomerase reverse transcriptase	Upregulated	Boltze et al. 2003
Heat shock protein 90	Upregulated	Boltze et al. 2003, Xu et al. 2013
Activator of transcription 3 (STAT3)	Increased	Xu et al. 2013
Vascular endothelial growth factor	Increased	Salmenkivi et al. 2003b
Tenascin	Increased	Salmenkivi et al. 2001a
Cyclooxygenase-2	Increased	Cadden et al. 2007, Saffar et al. 2011, Salmenkivi et al. 2001b
Inhibin α	Decreased	Salmenkivi et al. 2001c
C-erbB-2	Increased	Tavangar et al. 2010
Secretogranin II derived peptide	Decreased	Yon et al. 2003
SNAIL	Increased	Hayry et al. 2009
CD-44-S	Decreased	August et al. 2004
nm23	Decreased	Saffar et al. 2011
Galectin	Increased	Saffar et al. 2011

5.2.10. Posttranslational modifications of proteins

In nearly all proteins, during or after protein synthesis, covalent changes occur that modify protein conformation, stability, localization, and function (Xin and Radivojac 2012, Grammatikakis et al. 2017). In posttranslational modification, small chemical groups like methyl, phosphate, acetyl, lipids, carbohydrates, or other amino acids can be added or removed (Grammatikakis et al. 2017). One of the most complex posttranslational modifications is glycosylation of proteins (Lowe and Marth 2003). Unfavorable

posttranslational modifications can participate in tumorigenesis and malignant transformation (Grammatikakis et al. 2017).

Regulatory processes after mRNA transcription, posttranslational control, are an important part of gene expression control in eukaryotes and influence final protein levels. This control of mRNA metabolism enables cells to adapt quickly to changing environmental conditions (Garcia-Maurino et al. 2017). RNA-binding proteins (RBPs) are important factors in this regulation and posttranslational modifications occur also in RBPs. Human antigen R (HuR), also known as ELAVL1 (embryonic lethal abnormal vision-like 1), is an RBP which regulates many target mRNAs. Posttranslational modifications of HuR have an impact on its ability to bind target RNA and on its subcellular localization (Grammatikakis et al. 2017).

5.2.9.1 *Human antigen R and its target cyclooxygenase-2*

HuR is a product of the human *ELAV1* gene and a member of the ELAV / human antigen family, which has four members. HuR is expressed ubiquitously. HuB/Hel-N1, HuC, and HuD occur mainly in neuronal tissues (Wang et al. 2013b, Grammatikakis et al. 2017). HuR is an ARE-RBP that often binds transcripts in the 3´-untranslated region of eukaryotic mRNA at RNA stretches enriched in adenylate or uridylate (ARE = adenylate/uridylate rich element) (Garcia-Maurino et al. 2017; Grammatikakis et al. 2017). AREs are present in 5–8% of human genes (Garcia-Maurino et al. 2017). Many cancer-related genes, proto-oncogenes, tumor suppressors, antiapoptotic factors, growth factors, and cyclin-dependent kinase inhibitors are targets of HuR (Wang et al. 2013b) (Figure 5). HuR affects mainly the stability and transcription of mRNA but also targets pre-RNA splicing and nuclear export of mRNA (Grammatikakis et al. 2017). Final RNA expression will be affected by RBP competition for the same transcript and dynamic ARE-RBPs/mRNA interactions (Garcia-Maurino et al. 2017).

HuR has been associated with pathological conditions such as cancer, chronic inflammation, and cardiovascular and neurological disease. HuR is also involved in physiological processes like response to stress and immunoagents, adipogenesis, and muscle differentiation. The amount of HuR regulates its function, but mainly posttranslational mechanisms such as phosphorylation, methylation, and ubiquitination affect HuR function (Grammatikakis et al. 2017).

HuR consists of three RNA recognition motifs (RRMs). The first two domains (RRM1 and RRM2) bind RNA, and RRM3 is important for stability of the RNA-protein complex. Between RRM2 and RRM3 is a “hinge region” which contains the HuR nuclear shuttling domain, important for moving HuR from the nucleus to the cytoplasm and back. In unstimulated cells, HuR is mainly nuclear. In response to various stimuli, including mitogens and stress signals, HuR will be transported to the cytoplasm (Grammatikakis et al. 2017). Increased cytoplasmic HuR expression has been found in many malignant tumors, for example in glioblastomas and medulloblastomas (Nabors et al. 2001), in Merkel cell carcinoma (Koljonen et al. 2008), and in oral squamous cell carcinomas (Cha et al. 2011).

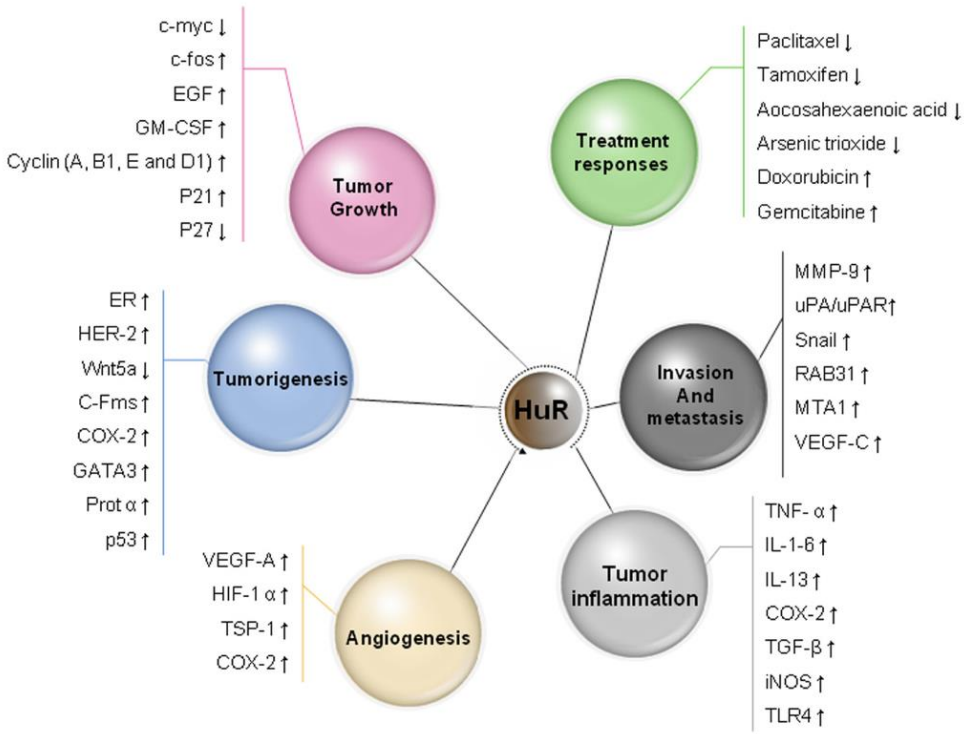

Figure 5. Diverse functions of human antigen R (HuR) in cancer development and progression through the regulation of stability or translation of target mRNAs that encode multiple cancer-related proteins. COX-2 = cyclooxygenase-2; EGF = epidermal growth factor; ER = estrogen receptor; GATA3 = trans-acting T-cell-specific transcription factor; GM-CSF = granulocyte-macrophage colony-stimulating factor; IL-6 = interleukin-6; IL-13 = interleukin-13; iNOS = inducible NO synthase; MMP-9 = matrix metalloproteinase-9; prot α = prothymosin α; TGF-β = transforming growth factor-β; TLR4 = toll-like receptor-4; TNF-α = tumor necrosis factor-α; TSP-1 = thrombospondin 1; uPA = urokinase-type plasminogen activator; uPAR = urokinase-type plasminogen activator receptor; VEGF = vascular endothelial growth factor (Wang et al. 2013b).

Cyclooxygenase-2

Cyclooxygenase-2 (COX-2), also known as prostaglandin-endoperoxide synthase 2, is a target of HuR. Cytoplasmic HuR expression is associated with high COX-2 expression in colorectal adenocarcinomas (Denkert et al. 2006), mucinous-type ovarian carcinomas (Erkinheimo et al. 2005), gastric cancer (Mrena et al. 2005), oral squamous cell carcinomas

(Cha et al. 2011), and non-small-cell lung carcinomas (Giaginis et al. 2015). COX-1 and COX-2 catalyze the initial step of prostanoid synthesis, i.e., prostaglandins and thromboxanes. Prostaglandins regulate different pathophysiological processes such as inflammatory reaction, renal hemodynamics, intestinal cytoprotection, hemostasis, and thrombosis. COX-1 is expressed constitutionally in most tissues and participates in prostaglandin production in normal physiological processes. COX-2 is inducible by various mitogenic and inflammatory stimuli. It is connected to the formation of carcinogens, angiogenesis, tumor promotion, inhibition of apoptosis, and metastatic process (Ghosh et al. 2010). Increased COX-2 levels have been reported in metastatic PHEOs and PGLs (Salmenkivi et al. 2001b, Cadden et al. 2007).

5.2.9.2 *Glycans*

Human cells are covered with glycans, which are carbohydrate units of glycoproteins, glycolipids, and proteoglycans. Glycan biosynthesis is a complex posttranslational event. About 1% of the human genome participates in it (Lowe and Marth 2003). The glycan structures have great variability, which leads to differences in biological and chemical properties. Glycosylation occurs mainly in the Golgi apparatus and endoplasmic reticulum but also in the nucleus and cytoplasm (Marth and Grewal 2008). Glycans can be divided into six principal families: 1) asparagine-linked (N-linked) glycans occurring mainly on glycoproteins, 2) serine- or threonine-linked (O-linked) glycans occurring mainly on membrane-bound mucins and glycoproteins, 3) glycosaminoglycans appearing as free polysaccharides or as part of proteoglycans, 4) glycosphingolipids, which consist of oligosaccharides binding to ceramide, 5) various nuclear and cytoplasmic proteins having O-linked N-acetylglucosamine, and 6) glycosylphosphatidylinositol-linked proteins (proteins which have a glycan linked to phosphatidylinositol) (Fuster and Esko 2005).

Glycans participate in important functions of intercellular signaling, cell adhesion, and cell motility (Marth and Grewal 2008). Alterations of these functions can lead to malignant transformation and can also be demonstrated as changes in cells' glycan profiles (Hakomori 1989, An et al. 2009). Some structural changes in glycans are associated with tumor aggressiveness, and on the other hand some structural alterations in glycans may serve as biomarkers in malignant tumors (Hakomori 1989, Okuyama et al. 2006, Arnold et al. 2008).

Changes in N-glycan structures have been identified in many cancers, for example lung (Satomaa et al. 2009a, Arnold et al. 2011), colorectal (Balog et al. 2012, Kaprio et al. 2015), and breast cancers (Abd Hamid et al. 2008). These cancer-associated N-glycan structures can participate in tumor growth (Girnita et al. 2000, Komatsu et al. 2001), angiogenesis (Pili et al. 1995), and invasion (Yoshimura et al. 1996, Granovsky et al. 2000).

6 Aims of the study

The major single aim of this thesis was to find biomarkers in PHEOs and PGLs for diagnostic, prognostic, and predictive purposes. A special focus has been on finding differentiating markers for metastatic and nonmetastatic tumors.

Detailed aims:

1. To study HuR protein expression and its prognostic relevance in PHEOs and PGLs.

2. To evaluate SSTR1–5 subtype profiles of PHEOs and PGLs, and possible associations of the SDHB status with the SSTR subtypes in these tumors.

3. To assess differences in N-glycosylation between nonmetastatic and metastatic PHEOs and PGLs.

4. To determine characteristics of thyroid PGLs, their frequency, histological and immunohistological characteristics, and genetic background.

7 Material and methods

7.1 Patient cohorts, tissue samples, and histopathological parameters

Studies I and II included consecutive patients with PHEO or PGL treated during years 1973–2009 at Helsinki University Hospital. Tissue samples from primary tumors were collected from the archives of the Department of Pathology, Helsinki University Hospital. The accuracy of diagnosis was verified. Clinical data were collected from hospital records and survival data from the Finnish Population Register Centre. The cause of death was obtained from Statistics Finland. The mean follow-up time was 14.2 years (median 13.9 years). Follow-up range for metastatic tumors was 0–41.1 years. One patient died during operation. For nonmetastatic tumors the follow-up range was 0.9–28.1 years. The patient with short follow-up died for reasons not related to the tumor.

In Study I the tumors were divided into three categories (Groups A–C) according to histopathological parameters. Group A consisted of nonmetastatic tumors without worrisome histology (n=70). Group B (n=68) included nonmetastatic tumors with histology including at least one of the following: tumor necrosis (sharply demarcated necrosis, possible signs of inflammation, and shadows of neoplastic cells), capsular (through the tumor capsule) and vascular invasion (in capsule or outside the tumor), and MIB1 ≥5%. Group C included 15 metastasized tumors of which 13 had a worrisome histology. From a patient with a metastatic disease, two PGLs were included in Study I, but in Study II only the tumor with worrisome histology was included. From Study II a patient was excluded who had MEN2 with adrenal tumor, which was in Study I, because following further consideration it suited better to the diagnosis hyperplasia of adrenal medulla than PHEO. The origin of four large tumors in the vicinity of the adrenals was reexamined from the operation protocols, and the organ adrenal based on pathological reports was changed to retroperitoneum in three of these four cases. PGLs constituted 16% of tumors. Of the 146 patients (Study II), 23 had a PGL and 123 a PHEO.

Study III included a subset of 16 patients, who were also included in Studies I and II. Eight patients had a metastatic disease and eight a nonmetastatic disease, eight had a PGL and eight a PHEO. In the metastatic group (Studies I–III), metastases were confirmed either histologically or radiologically by MIBG or SSTR scintigraphy.

Study IV included thyroid PGLs from a population-based European-American-Head-and-Neck-Paraganglioma-Registry, which is located in Freiburg, Germany. Eight patients in the registry were initially diagnosed as having a thyroid PGL but after reevaluation of the diagnoses morphologically and by IHC, five thyroid PGL diagnoses were confirmed. For all eight patients, registered demographic information was reevaluated and genetic testing performed. Table 8 and Figure 6 summarize the material in Studies I–IV.

Table 8. Tumor material in the original publications.

Study	I	II	III	IV
Patients	147	146	16	5
Pheochromocytomas	131	127	8	0
Paragangliomas	22	24	8	5
Tumors associated with metastatic disease	15	14	8	0

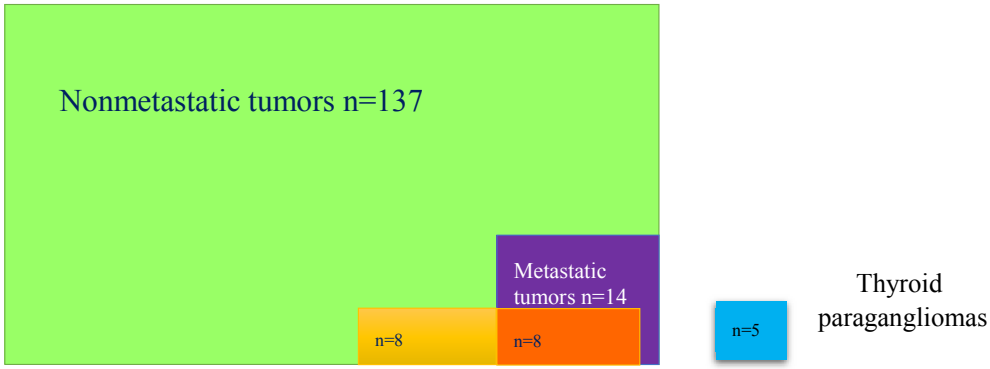

Figure 6. Patient cohorts in Studies II–IV. Study II: the metastatic tumors (n=14) are depicted in purple color and the nonmetastatic ones (n=137) in light green color. Study III: the metastatic tumors (n=8) are shown in dark orange and the nonmetastatic tumors ones (n=8) in light orange. Thyroid PGLs in Study IV (blue color) are a separate group. The areas are not in proportion to the size of the cohorts.

7.2 Tissue microarray blocks

For construction of tissue microarray (TMA) blocks (Studies I and II), H&E slides were reevaluated and representative areas from the primary tumors chosen. The chosen areas were located near the border of the tumors to ensure good fixation in the tumor cells. Only vital areas were chosen. Three 1 mm tumor punctures were drawn from analogous tissue

blocks and inserted into a recipient paraffin block with a semiautomatic tissue microarrayer (Beecher Instruments, Silver Spring, MD, MTABooster® Version 1.01 for Beecher Manual Arrayer, Alphelys). From each TMA block, one slide was cut to obtain three spots per tissue sample for immunohistochemical analysis. Proper sampling was controlled histologically by H&E and chromogranin A stainings.

7.3 Immunohistochemistry and scoring

The TMA blocks were cut into 4 μm thick sections and processed through deparaffinization in xylene followed by rehydration with graded alcohol series. The TMA slides were pretreated in a pretreatment module (LabVision UK Ltd, Suffolk, UK) with Tris-HCl buffer pH 8.5 for 20 min at 98°C (HuR19A12, HuR3A2, COX-2, MIB1, chromogranin A), with Tris-EDTA pH 9 for 25 min at 98°C (synaptophysin, cytokeratin-pan, TTF1, p53), with citrate buffer pH 6.0 for 25 min at 98°C (SSTR1, SSTR3-5) or no pretreatment done (S-100, calcitonin). SSTR2 antibody pretreatment was done with Cell Conditioning Solution (CC1) for 30 min in a Benchmark XT (Roche, Tucson, AZ, USA). Details of antibodies, dilutions, and scoring are shown in Table 9. A peroxidase-conjugated polymer kit Envision (Agilent, Santa Clara, CA, USA) was used to detect antigens in an Autostainer 480 (LabVision Thermo Scientific UK Ltd, Cheshire, UK), except for SSTR2 which was detected with an Optiview DAB kit in a Benchmark XT (Roche, Tucson, AZ, USA). Counterstaining was done with Mayer's Hematoxylin (Lillie's Modification) (Agilent, Santa Clara, CA, USA) and mounting with Eukitt® mounting medium (Sigma-Aldrich, St. Louis, MO, USA). Immunohistochemical stainings with SDHB antibody 21A11 (ABCAM, Cambridge, MA, USA) and SDHA antibody 5A11 (ABCAM) were done as previously described (Miettinen et al. 2014). Scoring was performed independently by two pathologists (J.H. and H.L. in Studies I and II, M.M. and H.L SDHB and SDHA IHC and J.A. and H.L. in Study IV) without any knowledge of the clinical data. Cases of disagreement required a consensus score. Colon adenocarcinoma was used as a positive control for HuR19F12, HuR3A2, and COX-2 stainings and pancreatic islet cells and small intestine neuroendocrine cells for SSTR1–5. Tissues not expressing these proteins like those from the kidney and liver were used as a negative control.

Table 9.
Details of the antibodies used and scoring.

Antibody	Study	Clone	Company	Dilution	Scoring used
Ki-67	I, II, III, IV	MIB1/M7240 monoclonal	Agilent	1:100	Percentage of positive tumor cells
HuR19F12	I	HuR19F12 monoclonal	Gift from Dr Furneaux, UCHC, Farmington, CT, USA	1:30 000	Intensity of staining 0=0, 1=weak, 2=moderate, 3=strong (both cytoplasmic and nuclear staining scored) (Leijon et al. 2016)
HuR3A2	I	HuR3A2 monoclonal	Santa Cruz Biotechnology	1:1500	Same as above
COX-2	I	COX-2 monoclonal	Cayman Chemical	1:100	Same as above, only cytoplasmic staining
SSTR1	II	sstr1 monoclonal	AbD Serotec	1:500	0=0 1<10%, weak cytoplasmic positivity 2≥10% weak cytoplasmic positivity 3=moderate cytoplasmic positivity 4=strong cytoplasmic positivity* (Modified from Elston et al. 2015)
SSTR2	II	UMB-1 monoclonal	Abcam	1:300	0=0 1<10%, not totally circumferential membrane positivity 2≥10% not totally circumferential membrane positivity 3=strong circumferential membrane positivity in 10–94% of tumor cells 4=strong circumferential positivity in ≥95% of tumor cells** (Modified from Elston et al. 2015)
SSTR3	II	UMB-5 monoclonal	Abcam	1:7000	Intensity of cytoplasmic staining 0=0 1=weak 2=moderate 3=strong If <10% of tumor cells positive, downgraded by one grade ***
SSTR4	II	sstr4 monoclonal	AbD Serotec	1:500	Same as SSTR1
SSTR5	II	sstr5 monoclonal	Bio-RAD	1:1000	0=0 1<10%, weak cytoplasmic positivity 2≥10% weak cytoplasmic positivity 3=moderate cytoplasmic or some membrane positivity 4=strong cytoplasmic positivity or membrane positivity* (Modified from Elston et al. 2015)
Chromogranin A	I, II, III, IV	Rabbit polyclonal	Agilent	1:2000	Positive/negative
SDHB	II, III	21A11 Mouse monoclonal	Abcam	1:1000	Positive/negative (Miettinen et al. 2014)
SDHA	II, III	5A11 Mouse monoclonal	Abcam	1:1000	Positive/negative (Miettinen et al. 2014)
Cytokeratin-pan	IV	AEI/AE3 M3515 Mouse monoclonal	DAKO	1:100	Positive/negative
Synaptophysin	IV	27G12 Mouse monoclonal	Novocastra	1:200	Positive/negative

Calcitonin	IV	A0576 Rabbit polyclonal	DAKO	1:2500	Positive/negative
S-100	IV	Z 0311 Rabbit polyclonal	DAKO	1:700	Positive/negative in sustentacular cells
TTF1	IV	SPT 24 Mouse monoclonal	Novocastra	1:100	Positive/negative
p53	IV	DO-7 Mouse monoclonal	DAKO	1:150	Positive/negative

* For statistics, the scores for SSTR1, 4, and 5 were grouped into three groups: negative (score 0 and 1), intermediate positive (score 2 and 3), and strong (score 4).

** For statistics, the SSTR2 scores were grouped into three groups: negative (score 0 and 1), intermediate positive (score 2), and strongly positive (score 3 and 4).

*** For statistics, the SSTR3 scores were grouped into three groups: negative (score 0), intermediate positive (score 1), and strong (score 2 and 3).

7.4 Mass spectrometric N-glycan profiling

From representative tumor areas of formalin-fixed, paraffin-embedded tissue blocks were punched samples with a volume of at least 1 mm^3 for mass spectrometric analysis. The samples were deparaffinized with xylene and with an ethanol–water series according to standard procedures. By peptide N-glycosidase F digestion, asparagine-linked glycans were detached from tissue glycoproteins and purified by a series of microscale solid-phase extraction steps as previously described (Kaprio et al. 2015). Acidic N-glycans were analyzed in negative ion linear mode as $[M-H]^-$ ions and neutral N-glycans in positive ion reflector mode as $[M+Na]^+$ ions. Based on their relative signal intensities, the relative molar quantity of neutral and acidic glycan components was assigned. The mass spectrometric raw data were processed into the current glycan profiles as in previously described protocols. The glycan profiles were normalized to 100% to allow comparison between samples (Satomaa et al. 2009a, b, Kaprio et al. 2015).

7.5 Genetic analysis

The patients in Study IV were tested for germ-line mutations of genes which have been associated with HNPGLs: *SDHA*, *SDHAF2*, *SDHB*, *SDHC*, *SDHD*, *VHL*, *RET*, *MAX*, and *TMEM127* (Neumann et al. 2004, Schiavi et al. 2005, Burnichon et al. 2010). The mutations in all exons were analyzed in these genes except for RET, for which exons 8, 10, 11, and

13–16 were studied. DNA for genetic studies was obtained from EDTA-anticoagulated whole blood. Bidirectional Sanger sequencing of the coding regions and splice sites of all genes was done. To find a deletion or duplication of the above-mentioned genes, multiplex ligation-dependent probe amplification analyses for *VHL*, *SDHB*, *SDHC*, *SDHD*, *SDHAF2*, *MAX*, and *SDHA* and semiquantitative multiplex polymerase chain reaction (PCR) for *TMEM127* were done. To clarify the extent of large deletions, break points were detected through quantitative real-time PCR gene-dosage determination and characterized by long-range PCR and nucleotide sequencing. The DNA variants were evaluated with three *in silico* analyses (SIFT, MutationTaster, PolyPhen). If at least two of the three software packages predicted the DNA variant to be damaging/pathogenic, they were considered to be probably pathogenic.

7.6 Statistical analysis

In Studies I and II, the chi-square test or Fisher's exact test when applicable were used for comparisons of immunohistochemical, histological, and clinicopathological variables. A *P* value less than 0.05 was regarded as statistically significant. Tumor size was compared between nonmetastasized and metastasized tumors using the Mann–Whitney test. Statistical analyses were performed with SPSS version 20.0 software (IBM SPSS Statistics, SPSS Inc., Chicago, IL, USA).

In Study III, m/z variables with all values equal to zero or with the total sum of the m/z values less than 1.5% were removed before importing the data into the software. Principal component analysis (PCA) was done using default parameters (analysis based on case-wise missing data deletion and correlations). To compare differences in the glycan structures between the nonmetastasized and metastasized tumors, the Mann–Whitney test was used. When a statistically significant difference was found via the Mann–Whitney test, the mean relative amounts of glycan structures, the standard errors of the mean, and the fold difference of the means between the groups were calculated. Error propagation served to assess standard error of the fold difference. Every test was two-sided. For multiplicity testing adjustment, the Benjamini–Hochberg procedure with the false positivity rate of 0.15 was used. Statistical analyses were performed with Statistica version 12.6 (StatSoft, Tulsa, OK, USA) and SPSS version 20.0.

7.7 Approvals

This study was approved by the local ethics committee (Dnro HUS 226/E6/06, extension TMK02 §66 17.4.2013) and the National Supervisory Authority of Welfare and Health (TEO Dnro 10041/06.01.03.01/2012).

8 Results

8.1 Clinical, histopathological data, and proliferation (Studies I and II)

In the cohort of 146 patients, 83 were female and 63 were male, and 13 patients (8.9%) had a metastatic disease. Of the patients with a metastatic disease, 10 were male and 3 were female. The metastasized tumors included nine PGLs and five PHEOs. Of the PHEOs 4% were metastatic and 38% of the PGLs. The mean tumor size in the metastatic group was 112 mm, and it was 65 mm in the nonmetastatic group. The metastatic tumors had a higher proliferation index and more frequently tumor necrosis (Table 10).

Of the patients, 8% were known to have MEN2, 3% NF1, 5% von Hippel–Lindau syndrome, and based on our results, of those with SDHB IHC, 10% had SDHx mutation. Eight patients were known to have multifocal disease. All these patients were syndromic. Three had MEN2, three known SDHB mutation, and two VHL.

Table 10. Differences in proliferation (MIB1), size, and frequency of tumor necrosis between the metastatic and nonmetastatic pheochromocytomas and paragangliomas.

	Nonmetastatic (n=137)	**Metastatic (n=14)**	***P* value**
Mean MIB1	1.6%	5.6%	$P<0.0001$*
Range of MIB1	0–9%	1–12%	
Mean size	65 mm	112 mm	$P<0.0001$**
Range of size	6–120 mm	45–192 mm	
Tumor necrosis	14/137	5/14	$P=0.023$*

*Fisher's exact test
**Mann–Whitney test

8.2 Immunohistochemistry results

8.2.1 *Human antigen R protein (Study I)*

Metastatic PHEOs and PGLs had significantly more cytoplasmic HuR protein staining than nonmetastatic tumors with both HuR antibodies used. Also COX-2 staining was increased in metastatic tumors. Cytoplasmic HuR staining was associated with COX-2 positivity (P<0.0001, Fisher's exact test) and high MIB1 values (P<0.0001, Fisher's exact test). The tumors with histologically worrisome features expressed significantly more cytoplasmic HuR19F12 protein than tumors without worrisome histology. The tumors with vascular invasion had also more cytoplasmic HuR19F12. The results are summarized in Table 11. Figure 7 visualizes the stronger cytoplasmic staining in metastasized PHEOs and PGLs with HuR19F12 antibody in comparison with nonmetastasized tumors.

Table 11. Comparison of the immunohistochemistry (IHC) findings between metastatic and nonmetastatic pheochromocytomas and paragangliomas and the association with histological parameters.

Antibody	***P* value**	**Result**
MIB1	<0.0001*	Higher proliferation in metastatic than in nonmetastatic tumors
HuR19F12 cytoplasmic	<0.0001*	Stronger IHC expression in metastatic tumors than in nonmetastatic tumors
HuR19F12 cytoplasmic	0.021*	More abundant IHC expression in tumors with vascular invasion
HuR19F12 cytoplasmic	0.004*	Stronger IHC expression in nonmetastatic tumors with one or more histologically worrisome feature versus tumors without such features
HuR3A2 cytoplasmic	<0.0001*	Stronger IHC expression in metastatic tumors than in nonmetastatic tumors
COX-2	<0.0001*	Stronger IHC expression in metastatic tumors than in nonmetastatic tumors

*Fisher's exact test

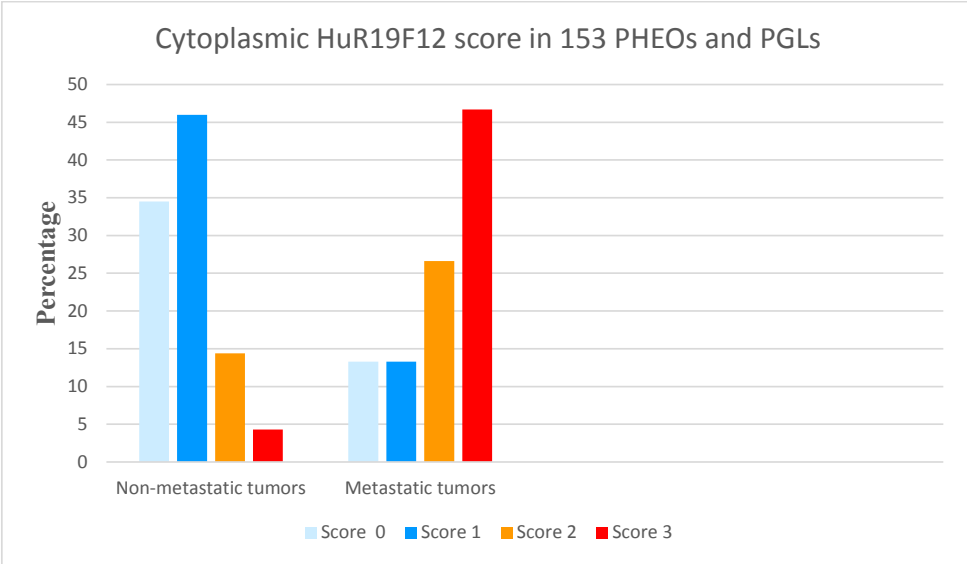

Figure 7. Comparison of immunohistochemical cytoplasmic HuR19F12 staining score (0–3) between nonmetastatic (n=139) and metastatic (n=15) pheochromocytomas (PHEOs) and paragangliomas (PGLs). The metastatic tumors express significantly more abundantly HuR19F12. (P<0.0001, Fisher's exact test.) HuR = human antigen R.

8.2.2 *Somatostatin receptors in pheochromocytomas and paragangliomas (Study II)*

151 primary PHEOs and PGLs were examined immunohistochemically with somatostatin receptor antibodies (SSTR1–5). The two most abundantly expressed somatostatin receptors were SSTR2 and 3. Table 12 shows SSTR1–5 expression in 151 PHEOs and PGLs including 14 metastatic tumors. SSTR1 expression was more abundant in PGLs than PHEOs (P=0.028, Fisher's exact test). Of PHEOs, 4.8% (6/125) showed weak SSTR4 positivity in >10% of tumor cells, while all PGLs were negative. With SSTR2, 3, and 5 antibodies no significant difference between PHEOs and PGLs existed.

Table 12. Immunohistochemical somatostatin receptor (SSTR1–5) expression in 151 pheochromocytomas (PHEOs) and paragangliomas (PGLs) including 14 metastatic tumors.

Antibody	PHEO			PGL			
	Negative	Inter-mediate positive	Strongly positive	Negative	Inter-mediate positive	Strongly positive	PHEO and PGL strongly positive total
SSTR1	86% (109/127)	14% (18/127)	0% 0	67% (16/24)	33% (8/24)	0% 0	0% 0
SSTR2	28% (35/127)	18% (23/127)	54% (69/127)	12% (3/24)	21% (5/24)	67% (16/24)	56% (85/151)
SSTR3	22% (28/127)	13% (17/127)	65% (82/127)	21% (5/24)	17% (4/24)	62% (15/24)	64% (97/151)
SSTR4	95% (119/125)	5% (6/125)	0% 0	100% (22/22)	0% 0	0% 0	0% 0
SSTR5	83% (106/127)	17% (21/127)	0% 0	92% (22/24)	8% (2/24%)	0% 0	0% 0

The scoring of immunohistochemistry has been described in Table 9.

8.2.2.1 *Somatostatin receptor expression in metastatic tumors*

Of the metastasized tumors, 10/14 were strongly SSTR2 positive (9 PGLs, 1 PHEO); thus the metastatic PGLs were expressing significantly more SSTR2 than the PHEOs (P=0.005, Fisher's exact test). Three metastatic PHEOs were completely SSTR2 negative (Table 13).

Metastatic tumors showed less SSTR3 positivity than nonmetastatic tumors (P=0.005). Among the metastatic tumors, 42.9% (6/14) were completely SSTR3 negative and 57.1% (8/14) intermediate or strongly positive, while of the nonmetastasized tumors 19.7% (27/137) showed no SSTR3 positivity and 80.3% (110/137) were intermediate or strongly positive. Also, tumors with high MIB1 value expressed less SSTR3. For other SSTR subtypes no differences between metastatic and nonmetastatic tumors emerged. However, metastatic tumors had individual variable SSTR profiles, which are shown in Table 13.

Table 13. Immunohistochemistry (IHC) staining results in 13 patients with metastatic pheochromocytomas and paragangliomas.

Gender and age (years) at diagnosis	Organ	SSTR1	SSTR2	SSTR3	SSTR4	SSTR5	SDHB IHC (+/−)
M 63	Retroperitoneum	N	S	I	N	N	+
F 57	Retroperitoneum (pancreas)	I	S	S	N	N	+
M 53	Retroperitoneum	N	S	I	N	I	−
F 46	Neck	N	S	N	N	N	−
F 24	Thorax year 1973	I	S	I	NA	N	−
The same patient as above	Retroperitoneum year 1998	N	S	N	N	N	−
M 31	Retroperitoneum	N	S	S	N	N	−
M 48	Retroperitoneum	I	S	N	N	N	−
M 39	Retroperitoneum	I	S	S	N	N	−
M 51	Adrenal	N	S	I	N	N	+
M 45	Adrenal	I	N	N	N	N	+
M 69	Adrenal	N	N	S	N	N	+
M 19	Adrenal	N	I	I	N	N	+
M 28	Adrenal	N	N	N	N	N	+

Abbreviations and color codes:
Somatostatin receptor (SSTR): S = strongly positive (red color); I = intermediate positive (orange color); N = negative (light yellow); NA = not available; SDHB = succinate dehydrogenase subunit B (SDHB): sufficient +, deficient −

8.2.3 *SDHB and SDHA immunohistochemistry expression (Studies II and III)*

Sixteen SDHB IHC negative primary tumors were found. They were all PGLs: 12 retroperitoneal, three thoracic, and one neck. Of the 146 patients, 15 (10.3%) had SDHB-negative tumors, and of the SDHB-deficient patients, 40% (6/15) had a metastatic disease. The patients who had SDHB-negative tumors were younger at diagnosis than the SDHB-positive patients. The median age of the SDHB-negative patients was 36 years (range 22–53 years) and that of the SDHB-positive patients was 53 years (range 17–87 years). SDHA-negative tumors were not found in this cohort. The SDHB status was not associated with IHC expression of SSTR1–5.

8.3 Glycomics (Study III)

N-glycans were analyzed in eight PHEOs and eight PGLs using matrix-assisted laser desorption/ionization time of flight mass spectrometric profiling. The N-glycan profiles were compared between metastasized (n=8) and nonmetastasized (n=8) tumors and between PHEOs (n=8) and PGLs (n=8). Both among acidic N-glycans and neutral N-glycans, we found more abundant fucosylation and complex fucosylation in metastatic PGLs and PHEOs than in nonmetastatic tumors. Among neutral N-glycans, also the hybrid-type N-glycans was more abundant in the metastatic group. The differences were statistically significant for individual tests, but when adjusted for multiplicity testing, they were above the false positive critical rate. Results for individual tests are in Table 14.

Table 14. Differences in neutral (A) and acidic (B) N-glycosylation between nonmetastasized and metastasized pheochromocytomas and paragangliomas.

A. Differences in neutral N-glycosylation between nonmetastasized and metastasized tumors.

Neutral N-glycan structures	**Ratio of mean ranks, metastasized/nonmetastasized**	**Ratio of means, metastasized/nonmetastasized**	***P* value***
Fucosylation	1.89	1.31	0.028
Complex fucosylation	1.75	1.90	0.049
Hybrid type	1.78	1.21	0.049

*Mann–Whitney test

B. Differences in acidic N-glycosylation between nonmetastasized and metastasized tumors.

Acidic N-glycan structures	Ratio of mean ranks, metastasized/nonmetastasized	Ratio of means, metastasized/nonmetastasized	*P* value*
Fucosylation	1.89	1.12	0.028
Complex fucosylation	1.81	1.91	0.038

*Mann–Whitney test

8.3.1 *Neutral and acidic asparagine-linked glycan profiles*

Neutral asparagine-linked glycan profiles
High-mannose type N-glycans were the five most abundant glycan signals, with compositions H5N2, H6N2, H7N2, H8N2, and H9N2. In metastatic tumors, four groups of **neutral N-glycan** signals were more abundant than in nonmetastatic tumors. Among these were 1) multifucosylated glycans, such as H4N3F2, H5N4F3, and H5N5F3; 2) a complex-type N-glycan signal that has been shown to indicate cancer-associated terminal N-acetylglucosamine; 3) hybrid-type N-glycans, such as H6N3F1; and also 4) fucosylated N-glycans such as H3N2F1, identified as paucimannose type based on their monosaccharide composition, were more abundant in metastatic tumors, whereas non-fucosylated paucimannose glycans such as H3N2 appeared more in nonmetastatic tumors.

Acidic asparagine-linked glycan profiles
Regarding acidic asparagine-linked glycan profiles, glycan signals composed of no or only one deoxyhexose residue (fucose), such as S1H5N4, S1H5N4F1, S2H5N4, and S2H5N4F1, occurred more in nonmetastasized tumors. In metastatic tumors, three groups of **acidic N-glycans** were more abundant: 1) multifucosylated N-glycans, such as S1H5N4F2 and S1H6N5F3; 2) acid ester-modified (sulfated or phosphorylated) glycans, such as H4N3F1P1, H3N4F1P1, and H4N5F2P1; and 3) hybrid-type/monoantennary N-glycans, such as S1H4N3F1.

8.3.2 *Principal component analysis*

PCA of the glycan profiling data could separate both the metastatic and nonmetastatic tumors and PGLs and PHEOs in distinct areas (visualized in Figure 8). The number in PCA corresponds to the patient number, whose characteristics are in Table 15.

Table 15. Characteristics of 16 patients with pheochromocytoma (PHEO) or paraganglioma (PGL) in Study III.

Patient	**Gender and age (years) at diagnosis**	**PHEO or PGL**	**Metastatic = M**	**Mutations (tested)**	**SDHB IHC +/−**	**Follow-up (years)**
1	M 19	PHEO	M	NF1	+	30
2	M 69	PHEO	M	ND	+	0
3	M 45	PHEO	M	ND	+	19
4	M 28	PHEO	M	No (VHL, RET, SDHB)	+	16
5	M 39	PGL	M	SDHB	−	15
6	M 48	PGL	M	ND	−	8
7	M 31	PGL	M	SDHB	−	21
8	F 57	PGL	M	No *	+	10
9	F 59	PHEO		No (RET)	+	7
10	F 57	PHEO		ND	+	10
11	M 50	PHEO		No (RET)	+	8
12	M 43	PHEO		No (RET)	+	9
13	F 34	PGL		SDHB	−	11
14	M 77	PGL		ND	+	3
15	M 48	PGL		SDHB	−	16
16	M 23	PGL		ND	−	16

*(MAX, VHL, NF1, REPRKAR1A, RET, SDHA, SDHAF2, SDHB, SDHC, SDHD, TMEM127)
Abbreviations: ND not determined SDHB, succinate dehydrogenase subunit B, sufficient +, deficient -.

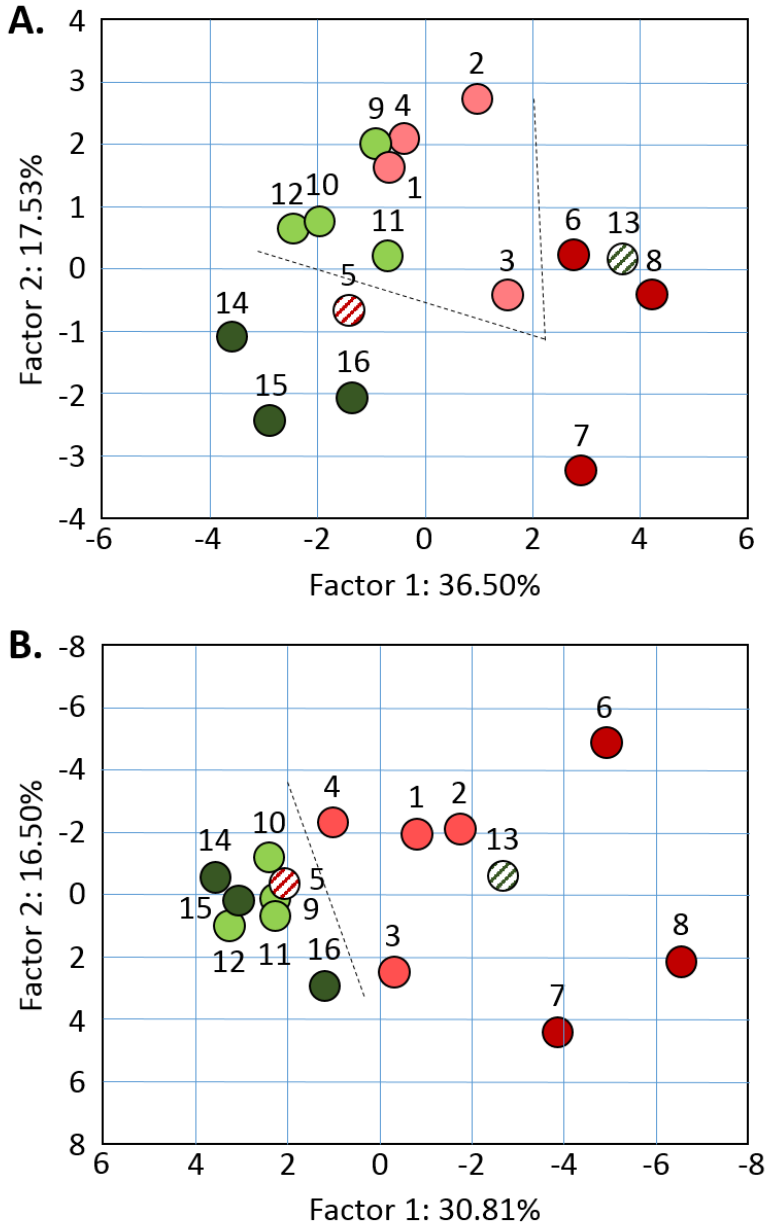

Figure 8. Differences in glycosylation of metastatic and nonmetastatic pheochromocytomas (PHEO) and paragangliomas (PGL) visualized in principal component analysis (PCA). Visualization of neutral (**A**) and combined neutral and acidic (**B**) N-glycan structures as PCA results on factor planes 1 and 2. The percentages indicate the amount of variance captured by each of the factors (1 or 2). Dotted lines illustrate the clustering of PHEOs and PGLs in neutral glycan PCA (**A**) and metastasized and nonmetastasized tumors in acidic and neutral glycan PCA (**B**). Light red, metastasized

PHEO; light green, nonmetastasized PHEO; dark red, metastasized PGL; dark green, nonmetastasized PGL. Numbers refer to the patient numbering in Table 15. Two SDHB-negative PGL tumors (5 and 13, marked with striped background) clustered with the opposite sample group (Leijon et al.2017)

8.4 Thyroid paragangliomas (Study IV)

8.4.1 *Clinical characteristics*

The prevalence of thyroid paraganglia was 0.5% (5/944) of all HNPGLs in the European-American-HNPGL-Registry. The clinical findings of five thyroid PGL patients are in Table 16. The age at diagnosis varied between 27 and 71 years, the median age being 40.6 years. Family history of SDHB mutation was known only in one patient (case 1). All patients underwent either total thyroidectomy or hemithyroidectomy. After a median follow-up of 5 years, no one had developed metastasis, but case 4, a 37-year-old female, had a recurrent PGL after the first operation.

Table 16. Demographic data for the five thyroid paraganglioma (PGL) patients.

Case	Gender and age (years)	Symptoms	FNA before operation	Initial diagnosis	Diagnosis PGL made	Mutation found in Study IV
1	M 27	A relative tested as SDHB positive	NA	PGL	After 1st operation	SDHB
2	M 32	Node in the neck	Adenoma	PGL	After 1st operation	SDHB
3	F 36	Node in the neck	NA	Hemangio pericytoma	After 3 years	SDHA
4	F 37	Lump in the neck	Follicular neoplasia	Follicular thyroid cancer	After 12 years	SDHA
5	F 71	Dysphagia	Follicular neoplasia	PGL	After 1st operation	Not in nine tested genes

FNA = fine-needle aspiration; NA = not available; SDHB = succinate dehydrogenase subunit B.

8.4.2 *Histology and immunohistochemistry in thyroid paragangliomas*

The histological and immunohistological findings were quite similar in all five thyroid PGLs. Morphology included fibrous septa and dense vascularization. The chief cells with clear or basophilic abundant cytoplasm formed nests (the classic Zellballen) and sheets. Some nuclear variation was seen and the mitotic rate was low. S-100 positive sustentacular cells were found as well.

In IHC stainings, chief cells were positive for chromogranin A and synaptophysin. Negative stainings were cytokeratin-pan, calcitonin, and TTF1. MIB1 was 3–5% and p53 was of wild type.

8.4.3 *Molecular genetic results*

Nine known predisposition genes for PGLs were analyzed: *SDHA*, *SDHAF2*, *SDHB*, *SDHC*, *SDHD*, *VHL*, *RET*, *MAX*, and *TMEM127*. Four out of five patients had germ-line DNA variants in the *SDHx* genes: two in the *SDHB* and two in the *SDHA* gene. A 27-year-old man had germ-line *SDHB* mutation c.664G>Ap.Arg177His. Eight of his 10 relatives were also mutation carriers, six having PGL or PHEO. Another 32-year-old male was found to have a complex rearrangement of the *SDHB* gene, consisting of a partial deletion of intron 2 and exon 3, and an Alu insertion. There were no additional PGLs in his family history. Two patients had germ-line DNA variants of the *SDHA* gene, which were probably mutations rather than polymorphisms according to silico analyses. No family history of PGLs could be found in these patients. All four patients with *SDHx* mutations were under 40 years of age when the diagnosis of thyroid PGL was made.

9 Discussion

PHEOs and PGLs constitute a rare and heterogeneous tumor group, with genetic, molecular, and histological variation and with differences in prognosis. Therefore, studies with these tumors are challenging to perform. Many studies have tried to find clinical, histological, or immunohistochemical biomarkers that are associated with aggressive behavior of PHEOs and PGLs. Although the knowledge of this tumor group has increased a lot during recent years, we still have no unequivocal widely accepted and validated means to predict the outcome of an individual PHEO or PGL.

Genetic factors and prognosis in pheochromocytomas and paragangliomas

The traditional 10% rule claiming that 10% of PHEOs are malignant, 10% bilateral, 10% extra-adrenal, and 10% hereditary does not apply anymore, as about 30–40% of tumors are known to have hereditary background (Pillai et al. 2016, Crona et al. 2017, Tischler et al. 2017). Our cohort of 153 consecutive PHEOs and PGLs with a long follow-up time and clinical data is comprehensive regarding the rarity of these tumors. PGLs constitute 16% of this cohort. Less than 10% of tumors were metastatic (4% of PHEOs and 38% of PGLs), which is less than reported. It is possible that some patients still develop metastases, as the latest tumors were operated in 2009, and late metastases occur. Some tumors with metastatic potential may have been diagnosed and operated radically before metastases occurred. The hereditary background in our cohort was not fully studied. The oldest tumors in this cohort were treated before genetic testing was common practice. However, 8% of the patients were known to have MEN2, 3% NF1, 5% von Hippel–Lindau syndrome, and based on our results of SDHB IHC, 10% were known to have *SDHx* mutation. Eight patients were known to have multifocal disease. All these patients were syndromic. Three had MEN2, three had known *SDHB* mutation, and two had VHL. Of *SDHB* mutation carriers' tumors, which mostly are PGLs, about 30% metastasize, and *SDHB* mutation is nowadays the strongest predictive factor of aggressive behavior of these tumors. In this Finnish cohort, 40% of the patients with immunohistochemically SDHB-negative tumors had metastatic disease. IHC is known to be a sensitive and specific method to identify SDHB mutation. No *SDHA* mutation was found. Knowledge of different genetic backgrounds and prognosis has increased, but it is by no means complete and probably new genes will be found. Individual targeted genetic testing is recommended for every PGL and PHEO patient. Identification of an inherited pathogenic mutation has clinical impact. It can lead to early diagnosis of multiple tumors and metastases in the patient and investigations of the relatives at risk. The genetic background has an impact on tumor pathogenesis. Thus, probably the same prognostic and predictive markers may not be valid for all PHEOs and PGLs.

With understanding the role of *SDHx* mutations, prediction of the metastatic potential of PHEOs and PGLs has become slightly more accurate; however, new prognostic markers are still needed. Location of the primary tumor plays a role as PGLs metastasize more often than PHEOs. This was true also in our material. In a study by Ayala-Ramirez et al. (2011)

comprising 290 tumors, the location of the primary tumor was a stronger predictor of metastases than the size in multivariate analysis, but metastatic PHEOs and PGLs were also larger than nonmetastatic ones. The mean size of the primary tumors of the metastatic neoplasms was 8.2 cm and that of the nonmetastatic ones 4.9 cm (Ayala-Ramirez et al. 2011). The size was important also in our study, in which the tumors were larger than in the study of Ayala-Ramirez. However, among the few metastasized cases we had one very large 19.5 cm PHEO which increased the mean metastasized tumor size. The smallest primary tumor associated with metastatic disease was 4.5 cm in diameter.

Basic histopathology and cell proliferation in diagnostic and prognostic evaluation of pheochromocytomas and paragangliomas

A high proliferation rate of tumor cells analyzed by counting mitosis or MIB1/Ki-67 has been associated with aggressive potential (August et al. 2004, de Wailly et al. 2012). In our cohort, metastasized tumors had higher MIB1 values. Despite the difference in the proliferation index between metastasized and nonmetastasized PHEOs and PGLs, over half of metastasized tumors had an MIB1 value below 5%. The highest MIB1 value in nonmetastasized tumors was 9%. Thus, high proliferation rate is only a single risk factor for metastatic disease and is not sufficient to predict the metastatic potential alone.

Histological parameters such as necrosis, invasion, and mitotic count have previously been shown to be associated with metastatic disease (Salmenkivi et al. 2003a). In our cohort, necrosis occurred significantly more often in the metastatic group. Necrosis is an important factor reflecting the aggressive potential of tumors, but alone it gives limited information of prognosis. Both capsular and vascular invasion were more frequent in our cohort in metastasized tumors, but the difference was not statistically significant. These parameters are included in the most commonly used score systems – the PASS and GAPP scores (Thompson 2002, Kimura et al. 2014a). Traditional histology does not give an answer as to how a single tumor will behave, but risk stratification of a PHEO or PGL is recommended (Tischler et al. 2017).

No consensus has been reached regarding an adequate scoring system, but it should probably combine different factors as proposed in the PASS and GAPP scores (Thompson 2002, Kimura et al. 2014a). The proposed scoring systems have many common factors, which have been shown to be associated with metastatic potential. The factors to be scored should have clear criteria to avoid intra- and interobserver variation. To keep the scoring practical in clinical practice, it should not be too complicated and should include only factors most strongly associated with the metastatic potential of PHEOs and PGLs. In our results, both necrosis and MIB1 were significantly associated with metastatic disease. Both are factors which have been shown to be associated with the aggressive potential of tumors also in other neoplasms like adrenal cortical tumors (Pennanen et al. 2015) and leiomyosarcomas. Because necrosis and proliferation as single parameters are associated with metastatic potential, they probably are important histological hints to the aggressiveness of the tumor. A novel scoring system of adrenal cortical tumors, the Helsinki score, estimates the aggressive potential of the tumor by the amount of proliferation and the existence of necrosis (Pennanen et al. 2015). Maybe a score including necrosis, proliferation rate, location, and SDHB status would be informative for the aggressiveness of PHEOs and PGLs.

PGLs can occur also in very rare locations. As a separate cohort, we studied thyroid PGLs. Because of the rarity of this tumor, the diagnosis can be challenging and IHC is needed to confirm the diagnosis. Initially eight cases with a diagnosis of thyroid PGL were included in the European-American-HNPGL-Registry. After morphological and immunohistochemical reevaluation, the diagnosis of thyroid PGL could be confirmed only in five cases. The number of patients was very low, but according to our findings thyroid PGLs are strongly associated with SDHx mutations. Two patients had germ-line *SDHB* mutations and two had *SDHA* mutations, but in one patient none of the tested mutations was found. Thyroid PGLs seem to have a rather indolent clinical behavior according to our results. During the 5 years of follow-up, no metastases evolved.

Human antigen R's role as a biomarker for pheochromocytomas and paragangliomas

HuR protein is an example of a biomarker that can serve as a prognostic marker. In our cohort the majority, but not all, metastatic tumors showed increased intracytoplasmic HuR positivity, while the majority of nonmetastatic tumors were negative or only weakly positive. This was a new observation. Differences in the PHEO- and PGL-associated genes and mutations, known to affect pathogenesis, could explain the differences in HuR expression in metastatic tumors. HuR is involved in very complex posttranslational regulation and it has many different targets. Some of its functions and targets are probably still unknown as are its interactions with other factors. In many malignancies, intracytoplasmic HuR expression has been shown to be increased, and in most works increased HuR expression has been shown to be associated with higher tumor stage and worse prognosis, but even contradictory results have been published. In a study by Costantino et al. (2009), pancreatic cancer patients with high cytoplasmic HuR had lower mortality probably because HuR enhances the efficacy of gemcitabine. In breast cancer, high HuR expression has also been associated with a better prognosis (Yuan et al. 2010). Among malignancies with increased HuR expression are epithelial malignancies like oral squamous cell carcinoma (Cha et al. 2011), colorectal adenocarcinoma (Denkert et al. 2006), and mucinous-type ovarian carcinoma (Erkinheimo et al. 2005). Also, a neuroendocrine skin tumor, Merkel cell carcinoma (Koljonen et al. 2008), and neural tumors medulloblastoma and glioblastoma have increased HuR expression (Nabors et al. 2001). In neural crest derived neuroendocrine PHEOs and PGLs, more abundant cytoplasmic HuR expression is associated with metastatic potential in our study. Because of heterogeneity of malignancies associated with increased HuR expression, HuR seems to be a shared and common posttranslational factor in malignant transformation. Drugs which could inhibit HuR would be tempting, but one should know thoroughly the targets of HuR, the end results of its interactions, and also its impact on physiological processes.

N-glycans in pheochromocytomas and paragangliomas

Both the effect of HuR and changes in glycan structures are posttranslational events which can participate in malignant transformation. Cancer-associated asparagine-linked glycan (N-glycan) structures are involved in tumor progression and growth. We analyzed N-glycan profiles of eight PHEOs and eight PGLs and found differences between metastatic and nonmetastatic tumors, which was new knowledge. In metastasized PHEOs and PGLs, complex-type N-glycan signals of cancer-associated terminal N-acetylglucosamine, were more abundant than in nonmetastasized tumors. Interestingly this N-glycan structure has been shown to be increased in other malignancies like breast, lung, kidney, ovary (Satomaa et al. 2009a), and colon cancer (Kaprio et al. 2015); thus it seems to be a shared factor in

the pathogenesis of many tumors. In metastasized PHEOs and PGLs, fucosylation and complex fucosylation were more common than in respective nonmetastasized tumors, which differs from rectal tumors in which complex fucosylation is more common in benign adenomas than in cancers. PCA could separate metastasized and nonmetastasized tumors, but also PHEOs and PGLs, which strengthens the idea that PHEOs and PGLs have differences in their biology and behavior. N-glycans can be measured in serum and used as antigens in IHC. Identifying N-glycans, which are associated with aggressive behavior of PHEOs and PGLs, can in the future give some diagnostic and prognostic biomarkers for these tumors.

Somatostatin receptors in pheochromocytomas and paragangliomas

Only limited treatment options are available for metastatic PHEOs and PGLs. With increasing knowledge of the genetic background and pathogenesis associated with different mutations, also new targeted therapies can be developed, which hopefully will open new possibilities to treat metastatic disease (Roman-Gonzalez and Jimenez 2017). SSTR analogs can be used in imaging and in PRRT treatment of these tumors. According to our IHC results, PHEOs and PGLs have variable individual SSTR profiles. With the development of new SSTR analogs with affinity to several SSTR receptors and increased experience and validation of new monoclonal SSTR antibodies, it is possible that IHC can assist in the selection of an adequate SSTR analog for imaging and treatment targeted to a suitable subgroup of these tumors. According to our results, metastatic PHEOs and PGLs had different SSTR2 expression, which is an additional difference between PHEOs and PGLs. The differences in tumors´ SSTR expression could influence treatment and imaging practices. Metastatic and actively proliferating tumors expressed less SSTR3 than nonmetastatic tumors. The loss of SSTR3 expression may give a hint of a tumor's aggressive behavior, but larger studies combining clinical information and long follow-up would be needed to investigate this.

Strengths and limitations of our study

A large consecutive tumor cohort with clinical data attached to it is a strength. Also, a new technical approach like glycomics is beneficial to this reseach. A long follow-up time as included in our study is also obligatory to find out the true nature of the tumors. A limitation is the relatively low number of metastatic tumors due to the rarity of these neoplasias. This does not allow us to intepret our results too strongly. Nationwide biobank research would be beneficial to increase the number of both metastatic and nonmetastatic cases. Also, international collaboration such as in the thyroid PGL work would be of interest and would make it possible to collect more representative cases of rare lesions. Studies I and II are based on TMA material, which has some limitations. Some tumors express proteins in a heterogeneous fashion. TMA spots represent only a minority of the tumor area, which can cause some bias in the results. On the other hand, a traditional whole slide of the tumor represents only a small part of the neoplasm too. Many methodological and technical problems and errors are possible in IHC. There may be variations in fixation time among the tumors, which can impact the staining results. Also, the IHC staining process has many steps, which all should be done in an optimal fashion to get reliable results. Estimating IHC staining results is to some extent subjective, and intra- and interobserver variation occur. Most biological processes are a continuum and choosing the cutoff points of IHC scores is somewhat artificial too. With IHC we can demonstrate the presence of a protein in tumor cells, but further investigation will be needed to know the biological relevance of the

finding. Studies combining broad clinical, long-term follow-up information and IHC results would be beneficial. For example, studies where somatostatin analog based imaging results, response to somatostatin analog based therapy, and SSTR staining results could be combined.

Future prospects

As the heterogeneity in genetic background and pathogenesis of PHEOs and PGLs continue to become more evident, more diagnostic and treatment options will become available. Targeted therapies will become available as well. Adequate biobank samples including collections of a large number of rare disease cases will play a key role in the future, and patients with rare tumors like PHEOs and PGLs should be recruited for research. As molecular testing is becoming essential, liquid biopsies and cell-free tumor DNA can perhaps be used for sreening, surveillance, and perhaps even in treatment decisions.

10 Conclusions

The main conclusion is that expression of HuR, SSTR subtype profile, and N-glycomic profile may be used as potential biomarkers in PHEOs and PGLs. However, prediction of the behavior of a single PHEO or PGL is still uncertain.

The specific conclusions of this thesis are:

1. The majority of metastatic PHEOs and PGLs express moderately to strongly intracytoplasmic HuR protein, while the majority of nonmetastatic tumors are negative or only weakly positive. Thus strong intracytoplasmic HuR expression can point to metastatic potential in these tumors.

2. The SSTR1–5 profile of PHEOs and PGLs is individual and variable with the strongest expression of SSTR2 and SSTR3. Metastatic PGLs were all SSTR2 positive, while most metastatic PHEOs were negative. SSTR3 expression was lower in metastatic and actively proliferating tumors. No association with SSTR subtypes and SDHB status was found.

3. Fucosylation and complex fucosylation are more common in metastatic than nonmetastatic PHEOs and PGLs. Four neutral N-glycan groups and three acidic N-glycan groups are associated with metastatic disease.

4. Thyroid PGLs are rare tumors which constitute about 0.5% of HNPGLs. They have a strong association with SDHx mutations. Thyroid PGLs have a similar histology and IHC profile to other PGLs. The metastatic potential of these tumors is very low.

11 Acknowledgments

This study was carried out at the Department of Pathology, University of Helsinki and HUSLAB. I am grateful to the former head of the Medicum department, Vice Rector, Professor Tom Böhling, for his great warm leadership, creating a supportive atmosphere, and the excellent research facilities. I am grateful to the head of the Pathology department Professor Olli Carpén, Professor Ari Ristimäki, and the former heads Professor (Emeritus) Veli-Pekka Lehto and Professor (Emeritus) Leif Andersson for providing excellent research facilities. I wish to thank the Head of Pathology, Docent Kaisa Salmenkivi, and the acting Head of Pathology, Docent Päivi Heikkilä, for HUSLAB's positive attitude toward research and the possibility to work with my thesis in HUSLAB during my specialist training and as a specialist

I wish to express my sincere gratitude to my supervisors Professor Caj Haglund, Professor Johanna Arola, and Docent Kaisa Salmenkivi. It has been a privilege to be supervised by experienced scientists. Caj's enthusiasm and positivity have helped forward this scientific journey. Johanna's passion for science, energy, and excellent skills in clinical pathology have been indispensable. The years spent working on this thesis have been educational in many ways.

I thank the reviewers, Professors Tuomo Karttunen and Raimo Voutilainen, who helped me to improve this thesis, for their constructive and encouraging comments, as well as dedicated and thorough review of this work.

My college and friend Jaana Hagström is warmly thanked. She always tried to find time for scoring IHC in her busy schedule. She was always encouraging and ready to help with all kinds of problems. I express my sincere thanks to Professor Hartmut P H Neumann for a very nice and fruitful collaboration. Tero Satomaa and Tuomas Kaprio deserve special thanks for their expertise with, and important contribution to, interesting glycomics. Professor Markku Miettinen's help with SDHB IHC was crucial. Johanna Louhimo is warmly thanked for her excellent statistical work. I wish to express my appreciation to Satu Remes for her competence regarding, and contribution to, antibody validation. Camilla Schalin-Jäntti and Hanna Mäenpää are thanked for their important clinical contribution to this thesis. Co-authors Ilkka Heiskanen, Timo Paavonen, Saara Metso, Annamari Heiskanen, and Jukka.O. Hiltunen are warmly thanked.

Skillful and dedicated laboratory technicians Eija Heiliö and Päivi Peltomäki are warmly acknowledged for all laboratory work and assistance with other things. Päivi Mulari-Matikainen is also thanked for her help.

I thank all my friends and colleagues in HUSLAB Meilahti and Jorvi for their help. I wish to express special thanks to Sonja Boyd for practical advice regarding my thesis and some technical help with figures. Olli Tynninen is warmly thanked for friendly technical help

with figures. My fellow teachers in pathology Mikko Mäyränpää and Liisa Myllykangas are thanked for their supportive attitude and good collaboration with teaching, as well as other junior and senior teachers.

I thank my parents Aini and Jorma, and my siblings Katriina and Kyösti and their families. I thank my friends Tanja and Taina for a long-lasting, warm, and precious friendship.

Most of all I am grateful to my family: Peter, Elisa, Teresa, and Sandra for their love, patience, and support. You are the light and joy of my everyday life.

This work has been financially supported by the Finnish Awarded Special State Subsidy VTR, the Finnish Cancer Foundation, the Sigrid Jusélius Foundation, and Finska Läkaresällskapet.

12 References

Abd Hamid UM, Royle L, Saldova R, Radcliffe CM, Harvey DJ, Storr SJ, Pardo M, Antrobus R, Chapman CJ, Zitzmann N, et al. 2008. A strategy to reveal potential glycan markers from serum glycoproteins associated with breast cancer progression. Glycobiology 18(12):1105-18.

Almuhaideb A, Papathanasiou N, Bomanji J. 2011. 18F-FDG PET/CT imaging in oncology. Ann Saudi Med 31(1):3-13.

Ambrosini V, Fani M, Fanti S, Forrer F, Maecke HR. 2011. Radiopeptide imaging and therapy in europe. J Nucl Med 52 Suppl 2:42S-55S.

An HJ, Kronewitter SR, de Leoz ML, Lebrilla CB. 2009. Glycomics and disease markers. Curr Opin Chem Biol 13(5-6):601-7.

Arnold JN, Saldova R, Hamid UM, Rudd PM. 2008. Evaluation of the serum N-linked glycome for the diagnosis of cancer and chronic inflammation. Proteomics 8(16):3284-93.

Arnold JN, Saldova R, Galligan MC, Murphy TB, Mimura-Kimura Y, Telford JE, Godwin AK, Rudd PM. 2011. Novel glycan biomarkers for the detection of lung cancer. J Proteome Res 10(4):1755-64.

August C, August K, Schroeder S, Bahn H, Hinze R, Baba HA, Kersting C, Buerger H. 2004. CGH and CD 44/MIB-1 immunohistochemistry are helpful to distinguish metastasized from nonmetastasized sporadic pheochromocytomas. Mod Pathol 17(9):1119-28.

Ayala-Ramirez M, Palmer JL, Hofmann MC, de la Cruz M, Moon BS, Waguespack SG, Habra MA, Jimenez C. 2013. Bone metastases and skeletal-related events in patients with malignant pheochromocytoma and sympathetic paraganglioma. J Clin Endocrinol Metab 98(4):1492-7.

Ayala-Ramirez M, Feng L, Habra MA, Rich T, Dickson PV, Perrier N, Phan A, Waguespack S, Patel S, Jimenez C. 2012. Clinical benefits of systemic chemotherapy for patients with metastatic pheochromocytomas or sympathetic extra-adrenal paragangliomas: Insights from the largest single-institutional experience. Cancer 118(11):2804-12.

Ayala-Ramirez M, Feng L, Johnson MM, Ejaz S, Habra MA, Rich T, Busaidy N, Cote GJ, Perrier N, Phan A, et al. 2011. Clinical risk factors for malignancy and overall survival in patients with pheochromocytomas and sympathetic paragangliomas: Primary tumor size and primary tumor location as prognostic indicators. J Clin Endocrinol Metab 96(3):717-25.

Baguet JP, Hammer L, Mazzuco TL, Chabre O, Mallion JM, Sturm N, Chaffanjon P. 2004. Circumstances of discovery of phaeochromocytoma: A retrospective study of 41 consecutive patients. Eur J Endocrinol 150(5):681-6.

Balog CI, Stavenhagen K, Fung WL, Koeleman CA, McDonnell LA, Verhoeven A, Mesker WE, Tollenaar RA, Deelder AM, Wuhrer M. 2012. N-glycosylation of colorectal cancer tissues: A liquid chromatography and mass spectrometry-based investigation. Mol Cell Proteomics 11(9):571-85.

Barczynski M, Konturek A, Nowak W. 2014. Randomized clinical trial of posterior retroperitoneoscopic adrenalectomy versus lateral transperitoneal laparoscopic adrenalectomy with a 5-year follow-up. Ann Surg 260(5):740,7; discussion 747-8.

Bausch B, Tischler AS, Schmid KW, Leijon H, Eng C, Neumann HPH. 2017. Max schottelius: Pioneer in pheochromocytoma. J Endocr Soc 1(7):957-64.

Baysal BE and Maher ER. 2015. 15 YEARS OF PARAGANGLIOMA: Genetics and mechanism of pheochromocytoma-paraganglioma syndromes characterized by germline SDHB and SDHD mutations. Endocr Relat Cancer 22(4): T71-82.

Benn DE, Robinson BG, Clifton-Bligh RJ. 2015. 15 YEARS OF PARAGANGLIOMA: Clinical manifestations of paraganglioma syndromes types 1-5. Endocr Relat Cancer 22(4): T91-103.

Berends AMA, Buitenwerf E, de Krijger RR, Veeger NJGM, van der Horst-Schrivers ANA, Links TP, Kerstens MN. 2018. Incidence of pheochromocytoma and sympathetic paraganglioma in the Netherlands: A nationwide study and systematic review. Eur J Intern Med 51: 68-73.

Blake MA, Kalra MK, Maher MM, Sahani DV, Sweeney AT, Mueller PR, Hahn PF, Boland GW. 2004. Pheochromocytoma: An imaging chameleon. Radiographics 24 Suppl 1: S87-99.

Blank A, Schmitt AM, Korpershoek E, van Nederveen F, Rudolph T, Weber N, Strebel RT, de Krijger R, Komminoth P, Perren A. 2010. SDHB loss predicts malignancy in pheochromocytomas/sympathethic paragangliomas, but not through hypoxia signalling. Endocr Relat Cancer 17(4):919-28.

Boltze C, Mundschenk J, Unger N, Schneider-Stock R, Peters B, Mawrin C, Hoang-Vu C, Roessner A, Lehnert H. 2003. Expression profile of the telomeric complex discriminates between benign and malignant pheochromocytoma. J Clin Endocrinol Metab 88(9):4280-6.

Burnichon N, Buffet A, Parfait B, Letouze E, Laurendeau I, Loriot C, Pasmant E, Abermil N, Valeyrie-Allanore L, Bertherat J, et al. 2012. Somatic NF1 inactivation is a frequent event in sporadic pheochromocytoma. Hum Mol Genet 21(26):5397-405.

Burnichon N, Briere JJ, Libe R, Vescovo L, Riviere J, Tissier F, Jouanno E, Jeunemaitre X, Benit P, Tzagoloff A, et al. 2010. SDHA is a tumor suppressor gene causing paraganglioma. Hum Mol Genet 19(15):3011-20.

Cadden IS, Atkinson AB, Johnston BT, Pogue K, Connolly R, McCance D, Ardill JE, Russell CF, McGinty A. 2007. Cyclooxygenase-2 expression correlates with phaeochromocytoma malignancy: Evidence for a bcl-2-dependent mechanism. Histopathology 51(6):743-51.

Castelblanco E, Gallel P, Ros S, Gatius S, Valls J, De-Cubas AA, Maliszewska A, Yebra-Pimentel MT, Menarguez J, Gamallo C, et al. 2012. Thyroid paraganglioma. report of 3 cases and description of an immunohistochemical profile useful in the differential diagnosis with medullary thyroid carcinoma, based on complementary DNA array results. Hum Pathol 43(7):1103-12.

Castellani MR, Seghezzi S, Chiesa C, Aliberti GL, Maccauro M, Seregni E, Orunesu E, Luksch R, Bombardieri E. 2010. (131)I-MIBG treatment of pheochromocytoma: Low versus intermediate activity regimens of therapy. Q J Nucl Med Mol Imaging 54(1):100-13.

Castinetti F, Taieb D, Henry JF, Walz M, Guerin C, Brue T, Conte-Devolx B, Neumann HP, Sebag F. 2016. MANAGEMENT OF ENDOCRINE DISEASE: Outcome of adrenal sparing surgery in heritable pheochromocytoma. Eur J Endocrinol 174(1): R9-18.

Castro-Vega LJ, Buffet A, De Cubas AA, Cascon A, Menara M, Khalifa E, Amar L, Azriel S, Bourdeau I, Chabre O, et al. 2014. Germline mutations in FH confer predisposition to malignant pheochromocytomas and paragangliomas. Hum Mol Genet 23(9):2440-6.

Cha JD, Li S, Cha IH. 2011. Association between expression of embryonic lethal abnormal vision-like protein HuR and cyclooxygenase-2 in oral squamous cell carcinoma. Head Neck 33(5):627-37.

Choi YM, Sung TY, Kim WG, Lee JJ, Ryu JS, Kim TY, Kim WB, Hong SJ, Song DE, Shong YK. 2015. Clinical course and prognostic factors in patients with malignant pheochromocytoma and paraganglioma: A single institution experience. J Surg Oncol 112(8):815-21.

Chrisoulidou A, Kaltsas G, Ilias I, Grossman AB. 2007. The diagnosis and management of malignant phaeochromocytoma and paraganglioma. Endocr Relat Cancer 14(3):569-85.

Costantino CL, Witkiewicz AK, Kuwano Y, Cozzitorto JA, Kennedy EP, Dasgupta A, Keen JC, Yeo CJ, Gorospe M, Brody JR. 2009. The role of HuR in gemcitabine efficacy in pancreatic cancer: HuR up-regulates the expression of the gemcitabine metabolizing enzyme deoxycytidine kinase. Cancer Res 69(11):4567-72.

Crona J, Taieb D, Pacak K. 2017. New perspectives on pheochromocytoma and paraganglioma: Toward a molecular classification. Endocr Rev 38(6):489-515.

Davison AS, Jones DM, Ruthven S, Helliwell T, Shore SL. 2018. Clinical evaluation and treatment of phaeochromocytoma. Ann Clin Biochem 55(1):34-48.

de Wailly P, Oragano L, Rade F, Beaulieu A, Arnault V, Levillain P, Kraimps JL. 2012. Malignant pheochromocytoma: New malignancy criteria. Langenbecks Arch Surg 397(2):239-46.

DeLellis R, Lloyd R, Heitz P, Charis E, editors. 2004. WHO classification: Pathology and genetics. Tumours of endocrine organs. Third edition ed. Lyon: IARCPress:pp.159-166.

Denkert C, Koch I, von Keyserlingk N, Noske A, Niesporek S, Dietel M, Weichert W. 2006. Expression of the ELAV-like protein HuR in human colon cancer: Association with tumor stage and cyclooxygenase-2. Mod Pathol 19(9):1261-9.

Dhir M, Li W, Hogg ME, Bartlett DL, Carty SE, McCoy KL, Challinor SM, Yip L. 2017. Clinical predictors of malignancy in patients with pheochromocytoma and paraganglioma. Ann Surg Oncol 24(12):3624-30.

Duet M, Guichard JP, Rizzo N, Boudiaf M, Herman P, Tran Ba Huy P. 2005. Are somatostatin analogs therapeutic alternatives in the management of head and neck paragangliomas? Laryngoscope 115(8):1381-4.

Eisenhofer G and Peitzsch M. 2014. Laboratory evaluation of pheochromocytoma and paraganglioma. Clin Chem 60(12):1486-99.

Eisenhofer G, Lenders JW, Siegert G, Bornstein SR, Friberg P, Milosevic D, Mannelli M, Linehan WM, Adams K, Timmers HJ, et al. 2012. Plasma methoxytyramine: A novel biomarker of metastatic pheochromocytoma and paraganglioma in relation to established risk factors of tumour size, location and SDHB mutation status. Eur J Cancer 48(11):1739-49.

Eisenhofer G, Lenders JW, Timmers H, Mannelli M, Grebe SK, Hofbauer LC, Bornstein SR, Tiebel O, Adams K, Bratslavsky G, et al. 2011. Measurements of plasma methoxytyramine, normetanephrine, and metanephrine as discriminators of different hereditary forms of pheochromocytoma. Clin Chem 57(3):411-20.

Elston MS, Meyer-Rochow GY, Conaglen HM, Clarkson A, Clifton-Bligh RJ, Conaglen JV, Gill AJ. 2015. Increased SSTR2A and SSTR3 expression in succinate dehydrogenase-deficient pheochromocytomas and paragangliomas. Hum Pathol 46(3):390-6.

Erickson D, Kudva YC, Ebersold MJ, Thompson GB, Grant CS, van Heerden JA, Young WF, Jr. 2001. Benign paragangliomas: Clinical presentation and treatment outcomes in 236 patients. J Clin Endocrinol Metab 86(11):5210-6.

Erkinheimo TL, Sivula A, Lassus H, Heinonen M, Furneaux H, Haglund C, Butzow R, Ristimaki A. 2005. Cytoplasmic HuR expression correlates with epithelial cancer cell but not with stromal cell cyclooxygenase-2 expression in mucinous ovarian carcinoma. Gynecol Oncol 99(1):14-9.

Favier J, Amar L, Gimenez-Roqueplo AP. 2015. Paraganglioma and phaeochromocytoma: From genetics to personalized medicine. Nat Rev Endocrinol 11(2):101-11.

Feng N, Zhang WY, Wu XT. 2009. Clinicopathological analysis of paraganglioma with literature review. World J Gastroenterol 15(24):3003-8.

Fishbein L and Nathanson KL. 2017. Pheochromocytoma and paraganglioma susceptibility genes: Estimating the associated risk of disease. JAMA Oncol 3(9):1212-3.

Fishbein L, Leshchiner I, Walter V, Danilova L, Robertson AG, Johnson AR, Lichtenberg TM, Murray BA, Ghayee HK, Else T, et al. 2017. Comprehensive molecular characterization of pheochromocytoma and paraganglioma. Cancer Cell 31(2):181-93.

Fuster MM and Esko JD. 2005. The sweet and sour of cancer: Glycans as novel therapeutic targets. Nat Rev Cancer 5(7):526-42.

Garcia-Maurino SM, Rivero-Rodriguez F, Velazquez-Cruz A, Hernandez-Vellisca M, Diaz-Quintana A, De la Rosa MA, Diaz-Moreno I. 2017. RNA binding protein regulation and cross-talk in the control of AU-rich mRNA fate. Front Mol Biosci 4:71.

Ghosh N, Chaki R, Mandal V, Mandal SC. 2010. COX-2 as a target for cancer chemotherapy. Pharmacol Rep 62(2):233-44.

Giaginis C, Alexandrou P, Tsoukalas N, Sfiniadakis I, Kavantzas N, Agapitos E, Patsouris E, Theocharis S. 2015. Hu-antigen receptor (HuR) and cyclooxygenase-2 (COX-2) expression in human non-small-cell lung carcinoma: Associations with clinicopathological parameters, tumor proliferative capacity and patients' survival. Tumour Biol 36(1):315-27.

Girnita L, Wang M, Xie Y, Nilsson G, Dricu A, Wejde J, Larsson O. 2000. Inhibition of N-linked glycosylation down-regulates insulin-like growth factor-1 receptor at the cell surface and kills ewing's sarcoma cells: Therapeutic implications. Anticancer Drug Des 15(1):67-72.

Grammatikakis I, Abdelmohsen K, Gorospe M. 2017. Posttranslational control of HuR function. Wiley Interdiscip Rev RNA 8(1):10.1002/wrna.1372. Epub 2016 Jun 16.

Granovsky M, Fata J, Pawling J, Muller WJ, Khokha R, Dennis JW. 2000. Suppression of tumor growth and metastasis in Mgat5-deficient mice. Nat Med 6(3):306-12.

Grossrubatscher E, Dalino P, Vignati F, Gambacorta M, Pugliese R, Boniardi M, Rossetti O, Marocchi A, Bertuzzi M, Loli P. 2006. The role of chromogranin A in the management of patients with phaeochromocytoma. Clin Endocrinol (Oxf) 65(3):287-93.

Gunawardane PTK and Grossman A. 2017. Phaeochromocytoma and paraganglioma. Adv Exp Med Biol 956:239-59.

Hadoux J, Favier J, Scoazec JY, Leboulleux S, Al Ghuzlan A, Caramella C, Deandreis D, Borget I, Loriot C, Chougnet C, et al. 2014. SDHB mutations are associated with response to temozolomide in patients with metastatic pheochromocytoma or paraganglioma. Int J Cancer 135(11):2711-20.

Hakomori S. 1989. Aberrant glycosylation in tumors and tumor-associated carbohydrate antigens. Adv Cancer Res 52:257-331.

Harari A, Inabnet WB, 3rd. 2011. Malignant pheochromocytoma: A review. Am J Surg 201(5):700-8.

Hayry V, Salmenkivi K, Arola J, Heikkila P, Haglund C, Sariola H. 2009. High frequency of SNAIL-expressing cells confirms and predicts metastatic potential of phaeochromocytoma. Endocr Relat Cancer 16(4):1211-8.

Hescot S, Leboulleux S, Amar L, Vezzosi D, Borget I, Bournaud-Salinas C, de la Fouchardiere C, Libe R, Do Cao C, Niccoli P, et al. 2013. One-year progression-free survival of therapy-naive patients with malignant pheochromocytoma and paraganglioma. J Clin Endocrinol Metab 98(10):4006-12.

Jimenez P, Tatsui C, Jessop A, Thosani S, Jimenez C. 2017. Treatment for malignant pheochromocytomas and paragangliomas: 5 years of progress. Curr Oncol Rep 19(12):83.

Jochmanova I, Zelinka T, Widimsky J, Jr, Pacak K. 2014. HIF signaling pathway in pheochromocytoma and other neuroendocrine tumors. Physiol Res 63 Suppl 2: S251-62.

Kaemmerer D, Trager T, Hoffmeister M, Sipos B, Hommann M, Sanger J, Schulz S, Lupp A. 2015. Inverse expression of somatostatin and CXCR4 chemokine receptors in gastroenteropancreatic neuroendocrine neoplasms of different malignancy. Oncotarget 6(29):27566-79.

Kaemmerer D, Sanger J, Arsenic R, D'Haese JG, Neumann J, Schmitt-Graeff A, Wirtz RM, Schulz S, Lupp A. 2017. Evaluation of somatostatin, CXCR4 chemokine and endothelin A receptor expression in a large set of paragangliomas. Oncotarget 8(52):89958-69.

Kaprio T, Satomaa T, Heiskanen A, Hokke CH, Deelder AM, Mustonen H, Hagstrom J, Carpen O, Saarinen J, Haglund C. 2015. N-glycomic profiling as a tool to separate rectal adenomas from carcinomas. Mol Cell Proteomics 14(2):277-88.

Kempna P and Fluck CE. 2008. Adrenal gland development and defects. Best Pract Res Clin Endocrinol Metab 22(1):77-93.

Kimura N, Takayanagi R, Takizawa N, Itagaki E, Katabami T, Kakoi N, Rakugi H, Ikeda Y, Tanabe A, Nigawara T, et al. 2014a. Pathological grading for predicting metastasis in phaeochromocytoma and paraganglioma. Endocr Relat Cancer 21(3):405-14.

Kimura N, Takekoshi K, Horii A, Morimoto R, Imai T, Oki Y, Saito T, Midorikawa S, Arao T, Sugisawa C, et al. 2014b. Clinicopathological study of SDHB mutation-related pheochromocytoma and sympathetic paraganglioma. Endocr Relat Cancer 21(3): L13-6.

Koljonen V, Bohling T, Haglund C, Ristimaki A. 2008. Expression of HuR in merkel cell carcinoma and in normal skin. J Cutan Pathol 35(1):10-4.

Komatsu M, Jepson S, Arango ME, Carothers Carraway CA, Carraway KL. 2001. Muc4/sialomucin complex, an intramembrane modulator of ErbB2/HER2/Neu, potentiates primary tumor growth and suppresses apoptosis in a xenotransplanted tumor. Oncogene 20(4):461-70.

Korner M. 2016. Specific biology of neuroendocrine tumors: Peptide receptors as molecular targets. Best Pract Res Clin Endocrinol Metab 30(1):19-31.

Lack EE. 2007. Tumors of the Adrenal Glands and Extra-Adrenal Paraganglia. AFIP Atlas of Tumor Pathology. Series 4, Fascicle 8, Washington, DC: American Registry of Pathology, p. 283 and p. 323

Lamarre-Cliche M, Gimenez-Roqueplo AP, Billaud E, Baudin E, Luton JP, Plouin PF. 2002. Effects of slow-release octreotide on urinary metanephrine excretion and plasma chromogranin A and

catecholamine levels in patients with malignant or recurrent phaeochromocytoma. Clin Endocrinol (Oxf) 57(5):629-34.

Lawrence MS, Stojanov P, Mermel CH, Robinson JT, Garraway LA, Golub TR, Meyerson M, Gabriel SB, Lander ES, Getz G. 2014. Discovery and saturation analysis of cancer genes across 21 tumour types. Nature 505(7484):495-501.

Leijon H, Kaprio T, Heiskanen A, Satomaa T, Hiltunen JO, Miettinen MM, Arola J, Haglund C. 2017. N-glycomic profiling of pheochromocytomas and paragangliomas separates metastatic and non-metastatic disease. J Clin Endocrinol Metab 102(11):3990-4000.

Leijon H, Salmenkivi K, Heiskanen I, Hagstrom J, Louhimo J, Heikkila P, Ristimaki A, Paavonen T, Metso S, Maenpaa H, et al. 2016. HuR in pheochromocytomas and paragangliomas - overexpression in verified malignant tumors. APMIS 124(9):757-63.

Lenders JW, Eisenhofer G, Mannelli M, Pacak K. 2005. Phaeochromocytoma. Lancet 366(9486):665-75.

Lenders JW, Duh QY, Eisenhofer G, Gimenez-Roqueplo AP, Grebe SK, Murad MH, Naruse M, Pacak K, Young WF, Jr, Endocrine Society. 2014. Pheochromocytoma and paraganglioma: An endocrine society clinical practice guideline. J Clin Endocrinol Metab 99(6):1915-42.

Lenders JWM and Eisenhofer G. 2017. Update on modern management of pheochromocytoma and paraganglioma. Endocrinol Metab (Seoul) 32(2):152-61.

Letouze E, Martinelli C, Loriot C, Burnichon N, Abermil N, Ottolenghi C, Janin M, Menara M, Nguyen AT, Benit P, et al. 2013. SDH mutations establish a hypermethylator phenotype in paraganglioma. Cancer Cell 23(6):739-52.

Loriot C, Burnichon N, Gadessaud N, Vescovo L, Amar L, Libe R, Bertherat J, Plouin PF, Jeunemaitre X, Gimenez-Roqueplo AP, et al. 2012. Epithelial to mesenchymal transition is activated in metastatic pheochromocytomas and paragangliomas caused by SDHB gene mutations. J Clin Endocrinol Metab 97(6):E954-62.

Love JS and Anderson PG. 2015. Endocrine system. In: Stevens & Lowe's Human histology.Fourth edition Mosby p 264-285.

Lowe JB and Marth JD. 2003. A genetic approach to mammalian glycan function. Annu Rev Biochem 72:643-91.

Luchetti A, Walsh D, Rodger F, Clark G, Martin T, Irving R, Sanna M, Yao M, Robledo M, Neumann HP, et al. 2015. Profiling of somatic mutations in phaeochromocytoma and paraganglioma by targeted next generation sequencing analysis. Int J Endocrinol 2015:138573.

Makis W, McCann K, McEwan AJ. 2015. The challenges of treating paraganglioma patients with (177)lu-DOTATATE PRRT: Catecholamine crises, tumor lysis syndrome and the need for modification of treatment protocols. Nucl Med Mol Imaging 49(3):223-30.

Marth JD and Grewal PK. 2008. Mammalian glycosylation in immunity. Nat Rev Immunol 8(11):874-87.

Martucci VL and Pacak K. 2014. Pheochromocytoma and paraganglioma: Diagnosis, genetics, management, and treatment. Curr Probl Cancer 38(1):7-41.

Martucci VL, Lorenzo ZG, Weintraub M, del Rivero J, Ling A, Merino M, Siddiqui M, Shuch B, Vourganti S, Linehan WM, et al. 2015. Association of urinary bladder paragangliomas with germline mutations in the SDHB and VHL genes. Urol Oncol 33(4):167 e13-e20.

Mescher AL. 2013. Adrenal glands. In: Junqueira`s basic histology text and atlas. Weitz, M, Kearns, B., editors. 13 th ed. The McGraw-Hill Companies:pp. 414-418.

Miettinen M, Sarlomo-Rikala M, McCue P, Czapiewski P, Langfort R, Waloszczyk P, Wazny K, Biernat W, Lasota J, Wang Z. 2014. Mapping of succinate dehydrogenase losses in 2258 epithelial neoplasms. Appl Immunohistochem Mol Morphol 22(1):31-6.

Mohd Slim MA, Yoong S, Wallace W, Gardiner K. 2015. A large mesenteric paraganglioma with lymphovascular invasion. BMJ Case Rep 2015:10.1136/bcr, 2015-209601.

Mrena J, Wiksten JP, Thiel A, Kokkola A, Pohjola L, Lundin J, Nordling S, Ristimaki A, Haglund C. 2005. Cyclooxygenase-2 is an independent prognostic factor in gastric cancer and its expression is regulated by the messenger RNA stability factor HuR. Clin Cancer Res 11(20):7362-8.

Mundschenk J, Unger N, Schulz S, Hollt V, Schulz S, Steinke R, Lehnert H. 2003. Somatostatin receptor subtypes in human pheochromocytoma: Subcellular expression pattern and functional relevance for octreotide scintigraphy. J Clin Endocrinol Metab 88(11):5150-7.

Nabors LB, Gillespie GY, Harkins L, King PH. 2001. HuR, a RNA stability factor, is expressed in malignant brain tumors and binds to adenine- and uridine-rich elements within the 3' untranslated regions of cytokine and angiogenic factor mRNAs. Cancer Res 61(5):2154-61.

Nastos K, Cheung VTF, Toumpanakis C, Navalkissoor S, Quigley AM, Caplin M, Khoo B. 2017. Peptide receptor radionuclide treatment and (131)I-MIBG in the management of patients with metastatic/progressive phaeochromocytomas and paragangliomas. J Surg Oncol 115(4):425-34.

Neumann HP, Pawlu C, Peczkowska M, Bausch B, McWhinney SR, Muresan M, Buchta M, Franke G, Klisch J, Bley TA, et al. 2004. Distinct clinical features of paraganglioma syndromes associated with SDHB and SDHD gene mutations. JAMA 292(8): 943-51.

Niemeijer ND, Alblas G, van Hulsteijn LT, Dekkers OM, Corssmit EP. 2014. Chemotherapy with cyclophosphamide, vincristine and dacarbazine for malignant paraganglioma and pheochromocytoma: Systematic review and meta-analysis. Clin Endocrinol (Oxf) 81(5): 642-51.

Nijhoff MF, Dekkers OM, Vleming LJ, Smit JW, Romijn JA, Pereira AM. 2009. ACTH-producing pheochromocytoma: Clinical considerations and concise review of the literature. Eur J Intern Med 20(7):682-5.

Okuyama N, Ide Y, Nakano M, Nakagawa T, Yamanaka K, Moriwaki K, Murata K, Ohigashi H, Yokoyama S, Eguchi H, et al. 2006. Fucosylated haptoglobin is a novel marker for pancreatic cancer: A detailed analysis of the oligosaccharide structure and a possible mechanism for fucosylation. Int J Cancer 118(11):2803-8.

Oshmyansky AR, Mahammedi A, Dackiw A, Ball DW, Schulick RD, Zeiger MA, Siegelman SS. 2013. Serendipity in the diagnosis of pheochromocytoma. J Comput Assist Tomogr 37(5):820-3.

Pacak K, Jochmanova I, Prodanov T, Yang C, Merino MJ, Fojo T, Prchal JT, Tischler AS, Lechan RM, Zhuang Z. 2013. New syndrome of paraganglioma and somatostatinoma associated with polycythemia. J Clin Oncol 31(13):1690-8.

Papathomas TG, Oudijk L, Persu A, Gill AJ, van Nederveen F, Tischler AS, Tissier F, Volante M, Matias-Guiu X, Smid M, et al. 2015. SDHB/SDHA immunohistochemistry in pheochromocytomas and paragangliomas: A multicenter interobserver variation analysis using virtual microscopy: A multinational study of the european network for the study of adrenal tumors (ENS@T). Mod Pathol 28(6):807-21.

Paronen J, Vaisanen M, Leijon H. 2013. Pheochromocytoma can be an insidious disease. Duodecim 129(22):2375-8.

Pennanen M, Heiskanen I, Sane T, Remes S, Mustonen H, Haglund C, Arola J. 2015. Helsinki score-a novel model for prediction of metastases in adrenocortical carcinomas. Hum Pathol 46(3):404–10.

Pili R, Chang J, Partis RA, Mueller RA, Chrest FJ, Passaniti A. 1995. The alpha-glucosidase I inhibitor castanospermine alters endothelial cell glycosylation, prevents angiogenesis, and inhibits tumor growth. Cancer Res 55(13):2920-6.

Pillai S, Gopalan V, Smith RA, Lam AK. 2016. Updates on the genetics and the clinical impacts on phaeochromocytoma and paraganglioma in the new era. Crit Rev Oncol Hematol 100:190-208.

Poyhonen M, Kytola S, Leisti J. 2000. Epidemiology of neurofibromatosis type 1 (NF1) in northern Finland. J Med Genet 37(8):632-6.

Reubi JC. 2003. Peptide receptors as molecular targets for cancer diagnosis and therapy. Endocr Rev 24(4):389-427.

Roman-Gonzalez A and Jimenez C. 2017. Malignant pheochromocytoma-paraganglioma: Pathogenesis, TNM staging, and current clinical trials. Curr Opin Endocrinol Diabetes Obes 24(3):174-83.

Ross IL and Louw GJ. 2015. Embryological and molecular development of the adrenal glands. Clin Anat 28(2):235-42.

Ross MH and Pawlina W. 2006. Adrenal glands. In: Histology A text and atlas with correlated cell and molecular biology. Fifth Edition. Lippincott Williams &Wilkins. pp. 706-15.

Ross MH and Pawlina W. 2016. Adrenal glands. In: Histology A text and atlas with correlated cell and molecular biology. Seventh Edition. Lippincott Williams &Wilkins. pp. 766-75

Saffar H, Sanii S, Heshmat R, Haghpanah V, Larijani B, Rajabiani A, Azimi S, Tavangar SM. 2011. Expression of galectin-3, nm-23, and cyclooxygenase-2 could potentially discriminate between benign and malignant pheochromocytoma. Am J Clin Pathol 135(3):454-60.

Said-Al-Naief N and Ojha J. 2008. Hereditary paraganglioma of the nasopharynx. Head Neck Pathol 2(4):272-8.

Salinas-La Rosa CM. 2015. Orbital paraganglioma and succinate dehydrogenase staining for genetic testing triage and prognosis. Ocul Oncol Pathol 2(1):36-9.

Salmenkivi K, Haglund C, Arola J, Heikkila P. 2001a. Increased expression of tenascin in pheochromocytomas correlates with malignancy. Am J Surg Pathol 25(11):1419-23.

Salmenkivi K, Heikkila P, Haglund C, Louhimo J, Arola J. 2003a. Lack of histologically suspicious features, proliferative activity, and p53 expression suggests benign diagnosis in phaeochromocytomas. Histopathology 43(1):62-71.

Salmenkivi K, Heikkila P, Liu J, Haglund C, Arola J. 2003b. VEGF in 105 pheochromocytomas: Enhanced expression correlates with malignant outcome. APMIS 111(4):458-64.

Salmenkivi K, Haglund C, Ristimaki A, Arola J, Heikkila P. 2001b. Increased expression of cyclooxygenase-2 in malignant pheochromocytomas. J Clin Endocrinol Metab 86(11):5615-9.

Salmenkivi K, Arola J, Voutilainen R, Ilvesmaki V, Haglund C, Kahri AI, Heikkila P, Liu J. 2001c. Inhibin/activin betaB-subunit expression in pheochromocytomas favors benign diagnosis. J Clin Endocrinol Metab 86(5):2231-5.

Sane T. 2009. Lisämunuaisen kasvaimet ja paraganglioomat. In: Endokrinologia. Välimäki M, Sane T, Dunkel L, editors. 2nd edition ed. Jyväskylä: Kustannus Oy Duodecim:pp. 435-452.

Satomaa T, Heiskanen A, Leonardsson I, Angstrom J, Olonen A, Blomqvist M, Salovuori N, Haglund C, Teneberg S, Natunen J, et al. 2009a. Analysis of the human cancer glycome identifies a novel group of tumor-associated N-acetylglucosamine glycan antigens. Cancer Res 69(14):5811-9.

Satomaa T, Heiskanen A, Mikkola M, Olsson C, Blomqvist M, Tiittanen M, Jaatinen T, Aitio O, Olonen A, Helin J, et al. 2009b. The N-glycome of human embryonic stem cells. BMC Cell Biol 10:42.

Schiavi F, Boedeker CC, Bausch B, Peczkowska M, Gomez CF, Strassburg T, Pawlu C, Buchta M, Salzmann M, Hoffmann MM, et al. 2005. Predictors and prevalence of paraganglioma syndrome associated with mutations of the SDHC gene. JAMA 294(16):2057-63.

Sonneland PR, Scheithauer BW, LeChago J, Crawford BG, Onofrio BM. 1986. Paraganglioma of the cauda equina region. clinicopathologic study of 31 cases with special reference to immunocytology and ultrastructure. Cancer 58(8):1720-35.

Tavangar SM, Shojaee A, Moradi Tabriz H, Haghpanah V, Larijani B, Heshmat R, Lashkari A, Azimi S. 2010. Immunohistochemical expression of Ki67, c-erbB-2, and c-kit antigens in benign and malignant pheochromocytoma. Pathol Res Pract 206(5):305-9.

Thomas RM, Ruel E, Shantavasinkul PC, Corsino L. 2015. Endocrine hypertension: An overview on the current etiopathogenesis and management options. World J Hypertens 5(2):14-27.

Thompson LD. 2002. Pheochromocytoma of the adrenal gland scaled score (PASS) to separate benign from malignant neoplasms: A clinicopathologic and immunophenotypic study of 100 cases. Am J Surg Pathol 26(5):551-66.

Thosani S, Ayala-Ramirez M, Roman-Gonzalez A, Zhou S, Thosani N, Bisanz A, Jimenez C. 2015. Constipation: An overlooked, unmanaged symptom of patients with pheochromocytoma and sympathetic paraganglioma. Eur J Endocrinol 173(3):377-87.

Timmers HJ, Kozupa A, Chen CC, Carrasquillo JA, Ling A, Eisenhofer G, Adams KT, Solis D, Lenders JW, Pacak K. 2007. Superiority of fluorodeoxyglucose positron emission tomography to other functional imaging techniques in the evaluation of metastatic SDHB-associated pheochromocytoma and paraganglioma. J Clin Oncol 25(16):2262-9.

Tischler AS. 2008. Pheochromocytoma and extra-adrenal paraganglioma: Updates. Arch Pathol Lab Med 132(8):1272-84.

Tischler AS, de Krijger RR, Gill A, Kawashima A, Kimura N, Komminoth P, Papathomas TG, Thompson LDR, Tissier F, Williams MD, Young W.F., et al. 2017. Pheochromocytoma, extra-adrenal paragangliomas. WHO Classification of Tumours of Endocrine Organs 4th Edition:pp.180-195.

Unger N, Serdiuk I, Sheu SY, Walz MK, Schulz S, Saeger W, Schmid KW, Mann K, Petersenn S. 2008. Immunohistochemical localization of somatostatin receptor subtypes in benign and malignant adrenal tumours. Clin Endocrinol (Oxf) 68(6):850-7.

van Gelder T, Verhoeven GT, de Jong P, Oei HY, Krenning EP, Vuzevski VD, van den Meiracker AH. 1995. Dopamine-producing paraganglioma not visualized by iodine-123-MIBG scintigraphy. J Nucl Med 36(4):620-2.

Vitale G, Dicitore A, Sciammarella C, Di Molfetta S, Rubino M, Faggiano A, Colao AAL. 2018. Pasireotide in the treatment of neuroendocrine tumors: A review of the literature. Endocr Relat Cancer 25(6): R351-R364.

von Dobschuetz E, Leijon H, Schalin-Jantti C, Schiavi F, Brauckhoff M, Peczkowska M, Spiazzi G, Dematte S, Cecchini ME, Sartorato P, et al. 2015. A registry-based study of thyroid paraganglioma: Histological and genetic characteristics. Endocr Relat Cancer 22(2):191-204.

Wang HH, Chen YL, Kao HL, Lin SC, Lee CH, Huang GS, Chang WC. 2013a. Extra-adrenal paraganglioma of the prostate. Can Urol Assoc J 7(5-6): E370-2.

Wang J, Guo Y, Chu H, Guan Y, Bi J, Wang B. 2013b. Multiple functions of the RNA-binding protein HuR in cancer progression, treatment responses and prognosis. Int J Mol Sci 14(5):10015-41.

Wang JG, Han J, Jiang T, Li YJ. 2015. Cardiac paragangliomas. J Card Surg 30(1):55-60.

Xin F and Radivojac P. 2012. Post-translational modifications induce significant yet not extreme changes to protein structure. Bioinformatics 28(22):2905-13.

Xu Y, Qi Y, Rui W, Zhu Y, Zhang C, Zhao J, Wei Q, Wu Y, Shen Z, Ning G. 2013. Expression and diagnostic relevance of heat shock protein 90 and signal transducer and activator of transcription 3 in malignant pheochromocytoma. J Clin Pathol 66(4):286-90.

Yang C, Zhuang Z, Fliedner SM, Shankavaram U, Sun MG, Bullova P, Zhu R, Elkahloun AG, Kourlas PJ, Merino M, et al. 2015. Germ-line PHD1 and PHD2 mutations detected in patients with pheochromocytoma/paraganglioma-polycythemia. J Mol Med (Berl) 93(1): 93-104.

Yi C, Han L, Yang R, Yu J. 2017. Paraganglioma of the renal pelvis: A case report and review of literature. Tumori 103(Suppl. 1):e47-9.

Yon L, Guillemot J, Montero-Hadjadje M, Grumolato L, Leprince J, Lefebvre H, Contesse V, Plouin PF, Vaudry H, Anouar Y. 2003. Identification of the secretogranin II-derived peptide EM66 in pheochromocytomas as a potential marker for discriminating benign versus malignant tumors. J Clin Endocrinol Metab 88(6):2579-85.

Yoshimura M, Ihara Y, Matsuzawa Y, Taniguchi N. 1996. Aberrant glycosylation of E-cadherin enhances cell-cell binding to suppress metastasis. J Biol Chem 271(23):13811-5.

Yuan Z, Sanders AJ, Ye L, Jiang WG. 2010. HuR, a key post-transcriptional regulator, and its implication in progression of breast cancer. Histol Histopathol 25(10):1331-40.

Zelinka T, Musil Z, Duskova J, Burton D, Merino MJ, Milosevic D, Widimsky J, Jr, Pacak K. 2011. Metastatic pheochromocytoma: Does the size and age matter? Eur J Clin Invest 41(10):1121-8.

Zhang L, Liao Q, Hu Y, Zhao Y. 2014. Paraganglioma of the pancreas: A potentially functional and malignant tumor. World J Surg Oncol 12:218

Zheng S, Cherniack AD, Dewal N, Moffitt RA, Danilova L, Murray BA, Lerario AM, Else T, Knijnenburg TA, Ciriello G, et al. 2016. Comprehensive pan-genomic characterization of adrenocortical carcinoma. Cancer Cell 29(5):723-36.